



BRNO UNIVERSITY OF TECHNOLOGY

VYSOKÉ UČENÍ TECHNICKÉ V BRNĚ

FACULTY OF ELECTRICAL ENGINEERING AND COMMUNICATION

FAKULTA ELEKTROTECHNIKY
A KOMUNIKAČNÍCH TECHNOLOGIÍ

DEPARTMENT OF BIOMEDICAL ENGINEERING

ÚSTAV BIOMEDICÍNSKÉHO INŽENÝRSTVÍ

DIRECTED EVOLUTION OF ENZYMES ON MICROFLUIDIC CHIP

ŘÍZENÁ EVOLUCE ENZYMŮ NA MIKROFLUIDNÍM ČIPU

BACHELOR'S THESIS

BAKALÁŘSKÁ PRÁCE

AUTHOR

AUTOR PRÁCE

Táňa Kohúteková

SUPERVISOR

VEDOUCÍ PRÁCE

prof. RNDr. Zbyněk Prokop, Ph.D.

BRNO 2023

Bachelor's Thesis

Bachelor's study program **Biomedical Technology and Bioinformatics**

Department of Biomedical Engineering

Student: Táňa Kohúteková

ID: 227228

**Year of
study:** 3

Academic year: 2022/23

TITLE OF THESIS:

Directed evolution of enzymes on microfluidic chip

INSTRUCTION:

1) Get acquainted and conduct a literature review about options and technical assembly for droplet sorting. 2) Get acquainted with microfluidic chip fabrication and manipulation with a microfluidic system. 3) Study construction of protein libraries and subsequent expression in a suitable expression system (bacterial cells). 4) Perform fabrication of microfluidic chips and optimize fluorescence-activated droplet sorting (FADS) system for sorting with chosen fluorescence detection assay (aminophenyl fluorescein – APF). 5) Perform screening and sorting in droplets using the APF. 6) Collect data from the FADS system and design a new file format for saving collected data in software already created in LabView. Analyse collected data. 7) Thoroughly discuss obtained results.

RECOMMENDED LITERATURE:

- [1] Payne et al. High-throughput screening by droplet microfluidics: perspective into key challenges and future prospects. *Lab Chip*, 2020, 20, 2247-2262
- [2] Neun et al. Ultrahigh throughput screening for enzyme function in droplets. *Methods in Enzymology*, 2020, 643, 317-343

**Date of project
specification:** 6.2.2023

**Deadline for
submission:** 29.5.2023

Supervisor: prof. RNDr. Zbyněk Prokop, Ph.D.

Consultant: Ing. Vratislav Čmiel, Ph.D.

doc. Ing. Jana Kolářová, Ph.D.

Chair of study program board

WARNING:

The author of the Bachelor's Thesis claims that by creating this thesis he/she did not infringe the rights of third persons and the personal and/or property rights of third persons were not subjected to derogatory treatment. The author is fully aware of the legal consequences of an infringement of provisions as per Section 11 and following of Act No 121/2000 Coll. on copyright and rights related to copyright and on amendments to some other laws (the Copyright Act) in the wording of subsequent directives including the possible criminal consequences as resulting from provisions of Part 2, Chapter VI, Article 4 of Criminal Code 40/2009 Coll.

ABSTRACT

This thesis focuses on the directed evolution of enzymes using Fluorescence-Activated Droplet Sorting (FADS) on a microfluidic chip. A new FADS system was constructed, validated for high-throughput optical detection of microfluidic droplets, and coupled with real-time dielectrophoretic sorting. The system was benchmarked using two different populations (DhaA31, anchLD-RLuc) of Haloalkane dehalogenases (HLD) expressed in *Escherichia coli* cells and one population of empty pDR9 vector in a ratio of 5:45:50, mimicking the protein library. The collected and analyzed sorting data show that the droplet intensities were recorded in the same proportion as the theoretical ratio. The library of HLD mutants with insertions and deletions was then sorted using the system to obtain 1 % of the variants with the highest activity and the results are reported. The FADS data analyzing system was programmed in LabVIEW bundled with Python, with functions for initial analysis, prediction of threshold voltage, validation and graphical interpretation of data, and final reporting of processes.

KEYWORDS

Library sorting, directed evolution, lab-on-chip, dehalogenase, FADS, microfluidics

ABSTRAKT

Tato práce se zaměřuje na řízenou evoluci enzymů pomocí fluorescenčně řízeného kapénkového třídění (ang. zkratka FADS) na mikrofluidním čipu. Byl sestaven nový třídící systém, který byl validován pro vysoce výkonnou optickou detekci mikrofluidních kapének spojenou s dielektrickým tříděním. Systém byl testován pomocí dvou různých (DhaA31, anchLD-RLuc) populací haloalkan dehalogenas (HLD) exprimovaných v buňkách *Escherichia coli* a jedné populace prázdného vektoru pDR9 v poměru 5:45:50, což imituje proteinovou knihovnu. Naměřená a analyzovaná data z experimentu ukazují, že intenzity kapek ve validačním experimentu byly zaznamenány v stejném poměru jako teoretický poměr. Poté byla knihovna HLD mutantů s insercemi a delecemi tříděna pomocí FADS, za účelem získání 1 % nejaktivnějších variant. Program pro analýzu dat pro FADS byl programován v prostředí LabVIEW s využitím jazyka Python, s funkcemi pro počáteční analýzu, predikci prahového napětí, validaci a grafickou interpretaci dat a konečnou zprávu o experimentu.

KLÍČOVÁ SLOVA

Třídění knihoven na čipu, řízená evoluce, dehalogenasy, mikrofluidika

ROZŠÍŘENÝ ABSTRAKT

Enzymy haloalkan dehalogenasy představují poměrně dobře prozkoumanou skupinu, která slouží jako model pro proteinové inženýrství. Substrátem jsou především halogen alkyly, které mohou představovat riziko pro životní prostředí i člověka, protože řada z nich je zdraví škodlivá a některé mohou být karcinogenní. Většina halogen alkanů je syntetického původu a v přírodě se tudíž nacházejí v kontaminovaných oblastech. Haloalkan dehalogenasy katalyzují hydrolytické štěpení mezi uhlíkem a halogenem. Tímto reakčním mechanismem vznikají pro člověka méně škodlivé produkty: příslušný alkohol, halid a proton.

Mikrofluidika přináší nové možnosti v analytických metodách. Zabývá se manipulací velmi malých objemů a její výhodou je automatizace a miniaturizace experimentů. V proteinovém inženýrství nachází využití při screeningových experimentech knihoven se sto tisíci až miliony různých mutantů. Enzymy dehalogenasy a luciferasy mají navzdory různým reakčním mechanismům stejného předka. Pomocí mutací předpokládaného předka proteinu lze přezkoumat vliv evoluce na vývoj enzymů.

Pro detekci přítomnosti halogenovaných substrátů a pro hodnocení jejich aktivity se používají různé detekční eseje. Mnohé z nich však obsahují toxické látky, které mohou být pro laboratorní personál při manipulaci nebezpečné, proto byla vyvinuta HOX esej. Jedná se o citlivou fluorescenční detekční esej s nízkým detekčním limitem a bez toxických látek. Její součástí je aminofenylfluorescein, fluorogenní indikátor, jehož produkt byl excitován světlem o vlnové délce 477 nm. Tato detekční esej byla využita při mikrofluidním experimentu.

Prostředím pro provádění experimentů jsou tzv. mikrofluidní čipy. Pro tento experiment byly metodou měkké litografie vyrobeny 2 typy čipů: čip pro generování kapének a třídící čip. Čipy byly vyrobeny z polydimethylsiloxanu (PDMS), který je průhledný, bio kompatibilní a levný. Zhotovené čipy a podložní mikroskopická skříčka byly aktivovány kyslíkovou plazmou, a jejich spojením vznikl funkční čip s kanálky pro proudění kapalin. Jelikož vznikající kapénky představují systém voda-v-oleji, tak nově vzniklé kanálky v čipu pro generování kapének byly hydrofobně modifikovány. Tato modifikace musela být optimalizována, jinak se při generování vzniklé kapénky spojovaly nebo vodná fáze s buňkami tekla po stěnách kanálků. Modifikace a kvalita kapének závisí také na typu a koncentraci surfaktantu v olejové fázi, typu silanizačního činidla, oleje, filtraci roztoků, čase a teplotě. Po optimalizaci byl fluorovaný olej HFE 7500 vyhodnocený jako vyhovující pro modifikaci i pro olejovou fázi, na rozdíl od oleje FC 40. Změna doby pro inkubaci čipu silanizačním činidlem neměla žádný vliv na vhodnou modifikaci kanálků. Optimální koncentrace surfaktantu 008 RAN byla stanovena na 1 %, vyšší koncentrace tvořily nestabilní kapénky různých velikostí.

Třídící čipy obsahují kromě vstupů a výstupů pro kapaliny také elektrody, na které je přiváděno napětí. Při výrobě čipů bylo nutno optimalizovat upevnění drátků a jejich správné vodivé napojení na elektrody a také zhodnotit vliv modifikace kanálků. Modifikace třídícího čipu vedla k občasnému nezvratnému ucpávání kanálků a občasnému proniknutí silanizačního roztoku do vstupů pro elektrody. Po vložení a natavení Fieldova kovu používaného pro vytvoření elektrod, bránil vniklý olej správnému propojení taveniny a kontaktních drátků uvnitř kanálku. Jelikož kapénky jsou po reinjekci dispergovány v oleji a PDMS je přirozeně hydrofobní, tak po experimentálním ověření bylo zjištěno, že třídící čipy není nutné dodatečně modifikovat. Tím se předešlo ucpávání kanálků a poškození elektrod. Vypadávání drátků a přerušení elektrod bylo eliminováno zvýšením tloušťky čipu, zvýšením množství roztaveného Fieldova kovu a zvětšením tloušťky drátů adekvátně k šířce vstupů na čipu.

Fluorescenčně aktivované kapénkové třídění proteinů zvyšuje rychlost na stovky až tisíce měření za sekundu. Nově postavená sestava pro třídění sestávala z invertního mikroskopu, na který byly po bocích připojeny vysokorychlostní a fluorescenční kamery. Ty sloužily ke kontrole generování kapének a pro kontrolu správné trajektorie kapének při dielektroforetickém třídění. Oleje se surfaktantem byly na čip přiváděny pomocí stříkačkových injekčních pump a kapénky po inkubaci se substrátem byly přiváděny pomocí tlakové pumpy. Fluorescence byla vybudena prostřednictvím laseru a emisní záření bylo měřeno pomocí fotonásobiče. Pozice a zaostření laserového paprsku bylo umožněno pomocí emise fluorescenční barvy a získání optimálního signálu na fotonásobiči. Signál z fotonásobiče se zpracovával pomocí programovatelného hradlového pole, kde byla intenzita fluorescence průběžně vyhodnocována a následně zobrazena v programu vytvořeném v prostředí LabView. V případě překročení prahové intenzity byla přes zesilovač posílána na čip série obdélníkových napěťových pulzů, které vedly k dielektroforéze a následnému přitažení kapénky směrem k elektrodám do samostatného kanálku pro zachycení variant s požadovanou aktivitou.

Knihovna je soubor plazmidů různých inzerčních a delečních mutací. Jde o modernější přístup, jelikož dosud byly častěji využívány substituční mutace. Bakteriální buňky *Escherichia coli* BL21(DE3) byly transformovány teplotním šokem (angl. Heat shock transformation). Pro kalibraci a ověření správnosti třídění systému byly kultivovány buňky produkující enzymy se známou aktivitou - ancestrální enzym ancHLD-RLuc vykazující nízkou aktivitu a enzym DhaA31 s vyšší aktivitou z těchto enzymů. Jako negativní kontrola byly použity buňky transformované prázdným plazmidem pIDR9 nekódující protein a tedy nevykazující aktivitu.

Transformované a indukované buňky s enzymy byly smíchány v následném

složení: 50 % prázdného plazmidu pIDR9, 45 % ancHLD-RLuc a 5 % DhaA31. Kapénky byly generovány po dobu 2 hodin do kónické skleněné vialky předplněné minerálním olejem. Z důvodu reakce eseje a substrátu s povrchem skleněné vialky byla provedena modifikace silanem pro dosažení hydrofóbního povrchu. Následovala 40 minutová inkubace mimo čip a to 1,4 mmol/l dibromethanem naředěným v oleji se surfaktantem. Po ní byly kapénky tříděny na třídícím čipu. Hranice třídění byla nastavena na 1,5 V. Po třídění byl vygenerován histogram a na základě něj bylo ověřeno, že naměřené intenzity odpovídají teoretickému poměru buněčných variant.

Po ověření systému byly buňky transformovány pomocí inzerční a deleční knihovny, která vznikla mutací ancestrálního proteinu. Experiment probíhal podobně jako u validační knihovny. Vodnou fází při generování tvořila HOX esej s buňkami, olejovou fází 1 % surfaktant ve fluorovaném oleji. Substrátem byl opět 1,4 mmol/l dibromethan, který se inkuboval s dropletami po dobu 40 minut.

Po předběžné analýze části naměřených dat (cca 2500 kapének) byl stanoven práh pro třídění kapének na hodnotu 0,57 V. Při těchto podmínkách bylo vytříděno cca 2000 kapének, které byly sbírány do sterilní vody. Tyto mutantní varianty byly následně amplifikovány navazující řetězovou polymerázovou reakcí a vybrané varianty byly sekvenovány.

Během optimalizace třídícího systému byl navržen nový ukládací formát a vyvinut software pro analýzu naměřených dat. Software pro ovládání experimentu využíval původně formát .acq k ukládání prostých dat. Ten byl nahrazen formátem .tdms, který je strukturovaným, binárním formátem vyvinutým společností National Instruments a široce uplatnitelným v prostředí LabView. Do tohoto formátu se pak zapisovaly údaje o zaznamenané intenzitě z fotonásobiče 1, předpřipravený sloupec pro ukládání intenzity z fotonásobiče 2 a záznam o dielektroforetických pulzech. Vedle prostých dat, byly do tohoto formátu záznamu ukládána i metadata o třídících a detekčních parametrech, nastavených průtocích a laseru, datu experimentu a jeho autorovi.

Tato data jsou načtena ve zmíněném analyzačním softwaru, kde byla použita pro výpočet „pre-třídících“ výsledků, kde byl pro uživatele na základě kratšího úseku naměřených dat z počátečního trvání třídění vypočten práh pro vytřídění zvoleného procentuálního množství kapének. Z tohoto výpočtu byla vygenerována i PDF zpráva s histogramem. Po skončení experimentu software nabízí uživateli možnost „po-třídící“ analýzy, kde se ze souborů načte třídící práh a program vypočítá vytříděné množství kapének. Opět z této analýzy byla vygenerována PDF zpráva se všemi údaji o experimentu.

KOHÚTEKOVÁ, Táňa. *Directed evolution of enzymes on a microfluidic chip*. Brno: Brno University of Technology, Fakulta elektrotechniky a komunikačních technologií, Ústav biomedicínského inženýrství, 2023, 88 p. Bachelor's Thesis. Advised by prof. RNDr. Zbyněk Prokop, Ph.D.

Author's Declaration

Author: Táňa Kohúteková
Author's ID: 227228
Paper type: Bachelor's Thesis
Academic year: 2022/23
Topic: Directed evolution of enzymes on a microfluidic chip

I declare that I have written this paper independently, under the guidance of the advisor and using exclusively the technical references and other sources of information cited in the paper and listed in the comprehensive bibliography at the end of the paper.

As the author, I furthermore declare that, with respect to the creation of this paper, I have not infringed any copyright or violated anyone's personal and/or ownership rights. In this context, I am fully aware of the consequences of breaking Regulation § 11 of the Copyright Act No. 121/2000 Coll. of the Czech Republic, as amended, and of any breach of rights related to intellectual property or introduced within amendments to relevant Acts such as the Intellectual Property Act or the Criminal Code, Act No. 40/2009 Coll. of the Czech Republic, Section 2, Head VI, Part 4.

Brno

.....

author's signature*

*The author signs only in the printed version.

ACKNOWLEDGEMENT

First and foremost, I would like to express my sincere gratitude to the whole team at Loschmidt Laboratories for their kind help and support. Special thanks to prof. RNDr. Zbyněk Prokop, Ph.D. and Mgr. David Kovář, Ph.D. for their valuable guidance during this project. I also want to thank Ing. Marika Majerová for optimization of amplification and PCR and Irena Halíková for guidance and help with cell production. Additionally, I would like to highlight the collaboration with ETH in Zurich, especially Dr. Stavros Stavarkis from deMello group. In addition, I would like to thank Ing. Vratislav Čmiel, Ph.D. for his suggestions and help.

I would also like to highlight truly exceptional people, my parents, my sister Soňa and my partner Dávid for their love and encouragement during my study. And finally I want to extend my thanks to my classmates from BTB for their priceless friendship and unconditional support.

Contents

Introduction	14
1 Haloalkane dehalogenases	15
1.1 Structure and activity	15
1.2 Occurrence and applications	15
2 Protein engineering	17
2.1 Fundamentals of directed evolution	17
2.2 Construction of libraries	18
2.3 Sensitive fluorescent detection assay	20
3 Microfluidic-powered directed evolution	22
3.1 Screening methods	22
3.2 Fluorescence-activated droplet sorting systems	23
3.3 Lab-on-chip technology	23
3.3.1 Soft lithography and chip fabrication	24
3.3.2 Microfluidic chip for droplet generation	25
3.3.3 Surface modification	26
3.3.4 Microfluidic chip for droplet sorting	26
3.4 Technical assembly for droplet sorting	27
4 Experimental part	29
4.1 Fluorescence-activated droplet sorting system	30
4.2 Fabrication of microfluidic chips	33
4.2.1 Optimization of droplet quality	33
4.2.2 Encapsulation chip	36
4.2.3 Sorting chip	36
4.3 Optimization of droplet sorting system	37
4.3.1 Encapsulation	38
4.3.2 Sorting	38
4.3.3 Laser focusing with fluorescent dye	39
4.4 Sorting experiment	40
4.4.1 Protein production	40
4.4.2 Reaction mixture	41
4.4.3 Software settings of the experiment	42

5 Results and discussion	43
5.1 Droplet quality optimization	43
5.2 Optimization of sorting chip fabrication	46
5.3 Software for data analysis	47
5.3.1 New saving format	47
5.3.2 Graphical User Interface	49
5.3.3 Steps of analysis	51
5.4 Analysis of FADS experimental data	53
5.4.1 Benchmark experiment with fluorescent dye	53
5.4.2 Benchmark experiment with mixture of known variants	54
5.4.3 InDel library sorting with 1,2-Dibromethane	55
Conclusion	57
Bibliography	58
Symbols and abbreviations	62
List of appendices	64
A Pre-sorting report from InDel sorting	65
B Post-sorting report from InDel sorting	67
C LabView-Python software documentation	69
D Electronic supplement	88
D.1 LV-Project	88
D.2 Reports	88

List of Figures

2.1	Schematic representation of directed evolution.	18
2.2	Schematic representation of the haloalkane dehalogenases detection with fluorescent detection HO-X assay.	20
3.1	Workflow of microfluidic chip fabrication.	25
3.2	Schematic representation of dielectrophoretic sorting on a chip.	26
3.3	Schematic representation of optical setup with one PMT.	28
4.1	Newly assembled setup used for droplet sorting - front view.	31
4.2	Newly assembled setup used for droplet sorting - back view.	32
4.3	Design of the encapsulation chip.	36
4.4	Design of the sorting chip.	37
4.5	In-house made reservoir for droplet reinjection.	39
5.1	Picture of wetting the channel of the microfluidic chip.	43
5.2	Picture of droplets generated in microfluidic chip hydrophobically modified with FOTS in FC 40 oil.	44
5.3	Picture of droplets generated in microfluidic chip hydrophobically modified with 1 % TCPS in HFE 7500 oil.	44
5.4	Images from the microscope depicting the process of gelatinization of droplets.	45
5.5	Glass vial with generated droplets.	45
5.6	Sorting chip after optimization of the fabrication process.	46
5.7	Droplet without and with applied dielectrophoretic pulse.	47
5.8	Graphical user interface of Cinderella Analyser.	49
5.9	Graphical user interface of Cinderella Analyser - highlighted missing values.	50
5.10	Block scheme of analyzing software.	51
5.11	Sample of signal measured with different concentrations of HPTS.	53
5.12	Histogram from benchmark experiment with proteins.	54
5.13	Histogram from InDel library sorting.	55

List of Tables

2.1	Bioinformatic tools	19
3.1	The comparison of protein sorting methods	22
4.1	List of components used in construction of Fluorescence Activated Droplet Sorting system.	29
4.2	List of used chemicals.	30
4.3	Combinations of oil and surfactant of different (w/w)concentration used for oil phase optimization.	34
4.4	Combinations used for optimising surface modification process.	35
4.5	Encapsulation parameters - flowrate settings	38
4.6	Sorting parameters - flowrate settings.	39
4.7	Sorting parameters.	42
5.1	Final parameters for hydrophobic modifications.	44
5.2	List of data stored in TDMS file from the experiment.	48

Introduction

Haloalkane dehalogenases (HLDs) are bacterial enzymes that catalyze the cleavage of the bond between carbon and halogen. Halogenated compounds are environmentally toxic, however, HLDs convert them into primary alcohol and halide, which are less harmful. With their broad substrate specificity of many chlorinated, brominated, and iodinated compounds and easy manipulation, they are widely used in biotechnological applications for biosensing and biodegradation.

Thanks to a large amount of detailed data about enzyme mechanisms and structures, HLDs became an enticing target for protein engineering. The main goal of either rational design or directed evolution is to improve their catalytic efficiency or to extend their substrate specificity. To achieve a noticeable improvement in an enzyme, there is a need for methods that allow high-throughput screening to be able to analyze large libraries of mutants. There are several methods used for library screenings, for example, experiments on microtiter plates or fluorescence-activated cell sorting (FACS) and fluorescence-activated droplet sorting (FADS). With the use of conventional biochemical methods, the process of characterization of activity would take several months or even years to complete. Microfluidics enables droplet screening and sorting with a frequency of 1 kHz, which means that the library with approximately 1 million mutants could be screened within a few hours.

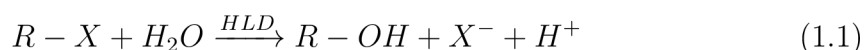
For this thesis, the FADS method is suitable for screening detection assay, because it enables the analysis of primary emulsions on a chip. In the case of FACS, the cells would have to produce an assay inside of cells or form a double emulsion system with the risk of droplet merging.

This thesis is focused on the development and optimization of the FADS system for the directed evolution of enzymes. The work involves conducting a literature review on options and technical assembly for droplet sorting, studying microfluidic chip fabrication and manipulation, construction of protein libraries and subsequent expression in bacterial cells. The newly assembled system was optimized for sorting with a halide detection assay. Screening and sorting were performed in droplets using the assay and the collected data were analyzed and discussed in detail. To facilitate data analysis, a new file format for saving the collected data in software already created in LabView was designed. Measured data were analyzed and processed in the program in LabView with functions from Python that also allowed a generation of PDF reports.

1 Haloalkane dehalogenases

1.1 Structure and activity

Haloalkane dehalogenases (HLD) belong to the class of α/β -hydrolases, which use water to cleave a bond between carbon and halogen. This family includes tens of thousands of proteins with a wide range of catalytic functions. Halogenated substrates are converted to respective alcohol, halides (halogen atoms with a negative charge), and protons [10]. The reaction mechanism of HLD is shown in equation 1.1.



Substrate specificity is a property of an enzyme that predisposes it to catalyze the transformation of certain substances. HLDs have broad substrate specificity with over one hundred halogenated compounds, which is the reason for many applications [30].

The structure of HLDs generally contains two domains – a main and a cap domain connected via loops. Domain in protein represents a separate structural unit responsible for specific functions. Both of them participate in the formation of the active site. The main domain contains 3 layers ($\alpha\beta\alpha$) composed of β -sheet of eight β -strands joined by six α -helices and it provides a scaffold for an active side. The cap domain consists of mostly helix structures and is flexible, so it enables change in shape and size of a tunnel leading to a change in the interaction of enzyme and substrate [12]. The tunnel provides access to the active site and ensures the binding and release of a substrate. Modification of the tunnel is one of the targets of protein modification to improve the activity.

1.2 Occurrence and applications

As chlorinated compounds are natural substrates for HLDs, bioremediation represents a propitious area of use. With the use of pesticides and herbicides in agriculture, substrates such as 1-chlorobutane or 1,2-dichloroethane are present in the environment. The reaction with HLDs was used in Lübeck in Germany to purify the water from 1,2-dichloroethane. It was possible to reduce concentrations from 2–15 mg/L to the final concentration of 0.01 mg/L with a rate of 5–20 m³/h [15].

Biosensing represents another interesting application as a good alternative to common methods such as gas chromatography (GC) and mass spectrometry

(MS) [15]. It comes with a shorter detection time and less restrictive thermostability and pH range. One of the biosensors for the detection of halogen derivatives and pollutants was EnviroPen invented in Enantis [7].

The last introduced application from many others is cell detection or protein labeling known as HaloTag. It was published by Los et al. in 2008 [19] and is commercialized by Promega Corporation. The method utilizes modified haloalkane dehalogenases with mutated catalytic histidine. This protein covalently binds synthetic ligands, which consist of a chloroalkane linker that reacts with the haloalkane dehalogenases and a functional group. This allows various functionalities to be introduced to the protein [19].

HLDs naturally occur in bacteria inhabiting contaminated environments and are involved in the biodegradation of pollutants. Besides them, HLDs are also present in eucaryotes, archaea, and marine organisms that are supposed to detoxify the environment polluted by the activity of sea algae [16].

Apart from their application in the field, they are also used in bioinformatics. They represent a well-researched model for protein engineering, which is a reason to increase the throughput of screening of different variants and their activity.

2 Protein engineering

Synthetic biology uses the capability of organic and biological chemistry to design non-natural molecules that are fully functioning in biological systems. It includes the design and construction of new biological systems and redesigning and even improving natural ones [14].

It represents a young field in biology and bioinformatics and yet achieves promising outcomes. Since the proteins, e.g., enzymes like HLDs, are widely used in pharmaceutical, biodegradation, and biosensing applications [15], demands are placed on efficiency and good yield of biocatalytic reactions by stating the rate-limiting step. HLDs that naturally occur in nature are slow and not specific, so there is an interest in improving them using protein engineering. This process includes three possible approaches: rational design, directed evolution, and semi-rational design. The rational design method uses the computer-aided design of protein with improved activity, thermal stability, or selectivity. It requires structural and functional knowledge about proteins to be able to predict how the change of a structure may influence properties. The data collection process takes several months and only after that it is possible to determine hot-spots – regions in protein structure that could be the target for mutagenesis. With the experimental data about the structure and function of a protein, only specific parts of a protein are selected for further mutagenesis. This approach represents the semi-rational design. On the other hand, directed evolution does not require any data before the experiment, but comes with bigger sizes of library.

2.1 Fundamentals of directed evolution

Directed evolution operates on the molecular level and takes advantage of random mutations of the selected protein. Unlike rational design, the only prerequisite of directed evolution is template deoxyribonucleic acid (DNA). By taking a protein from nature and introducing it to variability by mutagenesis, it is possible to create a library with over 10^6 mutations of a single protein. This process mimics a natural evolution but in a much shorter time [29].

Natural evolution takes a timescale of thousands of millions of years to evolve to a more developed protein, but with directed evolution, it can be shortened to weeks. As depicted in the schema in Fig. 2.1, naturally occurring protein is introduced to mutations, recombined, and sorted so that only the best remain and again introduced to mutations till the desired property is achieved [29].

Potentially disadvantageous is the size of the screened library – due to the random mutations within the sequence too many mutants need to be examined which is

expensive and takes a long time.

The analyzed gene from the parent protein is isolated and introduced to mutations, recombined, and transformed back into cells. By screening, it is possible to choose the best variants and get evolved genes. Evolved gene is used for another round of mutagenesis and sorting.

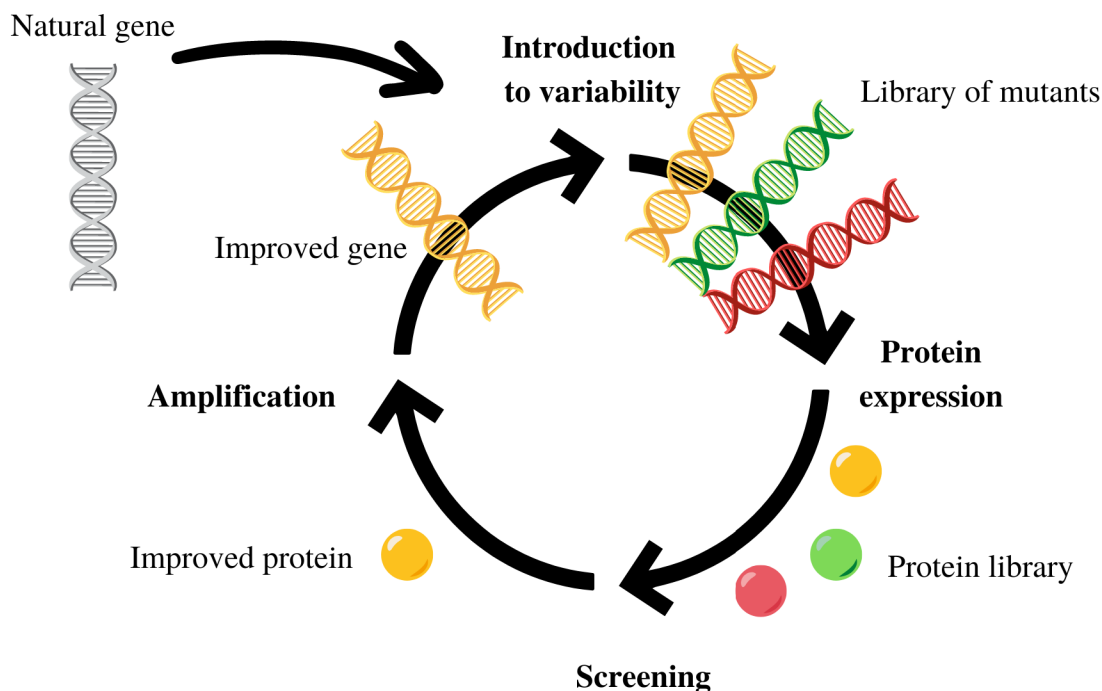


Fig. 2.1: Schematic representation of directed evolution.

2.2 Construction of libraries

In protein engineering, screening is a method for evaluating and choosing the best variant from mutants. The library is a set of multiple mutants of the examined protein. Screening of a library can be done by evaluating usually optical properties of a system, such as absorbance or fluorescence. According to the type of mutation, 2 different types of libraries exist: substitutional and insertion and deletion library (InDel). Substitutional libraries are more common in the field of protein engineering broadly used in directed evolution. The less information is known about examined protein, the bigger the library for screening needs to be. The biggest screened libraries have around 10^{15} mutants. Nowadays, the construction of smart protein libraries requires a precise selection of hot-spots to ensure diversity but also keep

the size relatively small. Design should have a high probability of getting improved protein and shorter screening time [2].

The close connection between protein engineering and bioinformatics led to several methods for the design and construction of libraries. Usually, amino acids that are responsible for substrate binding or product release are selected as hot-spots. Bioinformatics tools differ according to the purpose. An overview of bioinformatic tools and their purposes is shown in Tab. 2.1.

Tab. 2.1: Bioinformatic tools for protein engineering and their focus

Focus	Bioinformatic tool
Thermostability	FireProt, FRESCO
Evaluation of hot-spots	HotspotWizard

After precise library design, the library is constructed using several molecular methods, for example, polymerase chain reaction (PCR). PCR allows multiplying specific parts of DNA by repeated denaturation and renaturation with specific primers that determine the origin of replication.

Other mutations, such as insertions and deletions, can also have a strong impact on the properties of the enzyme and are very frequent in natural evolution. They are naturally caused by replication slippage when DNA polymerase sometimes pauses and dissociates from DNA during replication. Currently synthesized strand slips out and reanneals to the homologous part of the template in a different location. After the DNA resumes replication, one extra nucleotide is copied onto a new strand, or one is missing. Sometimes InDel mutations lead to a change of reading frame, which causes 66 % of mutation to be non-functional, but fortunately, some biological methods allow scientists to avoid it [21]. InDel mutations usually result in stronger purifying selection than substitution due to possible changes with a harmful impact on stability and other enzyme properties [22].

In molecular biology, a method called Random insertion and deletion (RID) mutagenesis was described in the early 2000s [21]. It allows to insert or delete any number of bases at any position. Targeted DNA is converted into a single strand DNA (ssDNA). Ce(IV)/EDTA complex is added to ssDNA and acts as molecular scissors. Other methods for the construction of such libraries include InDel assembly or transposon-based mutagenesis approach TRIAD [22].

The anchILD-RLuc protein is an ancestral protein that has both dehalogenase and luciferase activity. It is a reconstruction of a presumed ancestor. To screen both activities, the InDel library was created by the previously mentioned TRIAD

method either with only insertions or deletions. Construction of the library and screening of luciferase activity was previously reported [22], however, the evolution of dehalogenase activity is still waiting to be revealed. The library is used for describing the evolution of enzymes in nature. The goal would be to obtain the most active mutants with dehalogenase activity.

2.3 Sensitive fluorescent detection assay

To study the process of enzymatic dehalogenation of HLDs sensitive halide assays are used. According to the reaction in Equation 1.1, one of the products of dehalogenation is corresponding alcohol, which could be detected in Gas chromatography (GC) or Mass Spectrometry (MS) but with insufficient throughput. An increase in throughput was made by the detection of protons or halide ions, which are other products of dehalogenation.

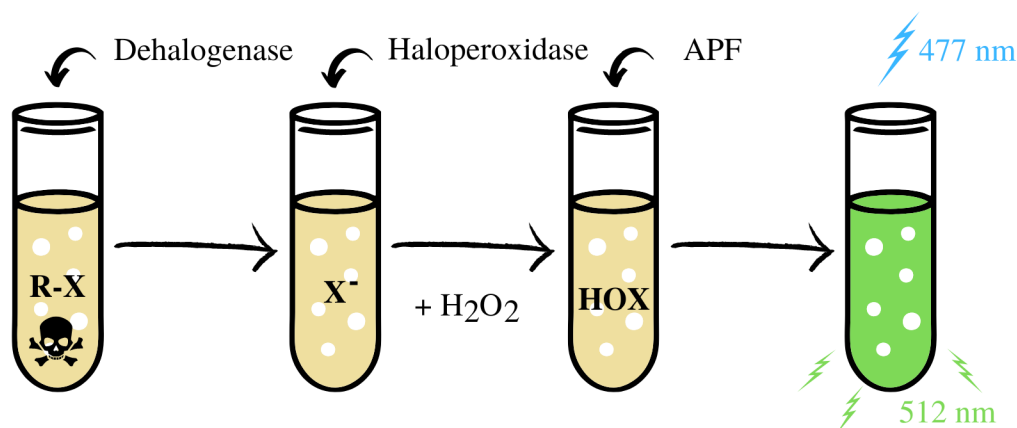


Fig. 2.2: Schematic representation of the haloalkane dehalogenases detection with fluorescent detection HO-X assay, adapted from [3];

R-X: Haloalkane, X: Halide, APF: Aminophenyl fluorescein, HOX: Hypohalous acid

For example, the Iwasaki assay, a colorimetric method for halide detection, is based on the detection of halide ions that are products of the reaction. Even though the assay enables the detection of low concentrations of chloride, it consists of mercuric thiocyanate [13] which is harmful to lab workers. Another option for halogen detection is based on the haloperoxidase-catalyzed oxidation of chloride, iodine, and bromide.

Halides are not generally reactive; however, they can be activated and detected by haloperoxidase-catalyzed oxidation. The cofactor in this case is a vanadate (V^{5+}) ion and it cycles between the vanadate and peroxovanadate form, which is oxidated.

Peroxovanade reacts with the halide ion and a proton and forms an intermediate that reacts with water to release the hypohalous acid (HO-X). Hydrogen peroxide re-oxidizes the vanadate to peroxovanadate, completing the haloperoxidase catalytic cycle. Aminophenyl fluorescein (APF) in reaction with hypohalous acid results in the formation of fluorescein - a bright fluorescent dye that can be detected at low concentrations. It requires to be excited with light at 477 nm and emits light at wavelength 512 nm [3]. The whole process is schematically illustrated in Fig. 2.2.

3 Microfluidic-powered directed evolution

Microfluidics and lab-on-chip (LOC) represents a new approach to studying cells, proteins, or pharmacological products. The main motivation was to significantly reduce the volumes of samples and to increase the throughput of experiments. In such small devices, the precision of control is also increased. Devices used in microfluidics are usually in the order of tens or hundreds of micrometers [25]. High throughput, with approximately 100 000 experiments per hour, enables the collection of large functional data sets for artificial intelligence training.

Microfluidics started with the miniaturization of analytical methods. In the 1970s the first miniature gas chromatographic air analyzer was built using photolithography [26]. Since then, this field came to the fore and nowadays is used broadly either as platforms or LOC.

3.1 Screening methods

Protein screening is a process of separating protein variants with desired properties, for example, activity or stability.

There are several conventional methods for screening but the throughput of variants that can be analyzed is several times smaller than the size of the library. Those methods include the use of microtitre plates or robotic stations. Some examples and comparisons concerning the volume and number of samples screened per day are in Tab. 3.1.

Tab. 3.1: The comparison of protein sorting methods [17][27]

Method	Sample volume [μL]	Library size
Agar plate	10^4	10^5
Microtitre plate	10^4	10^2
Microfluidic chip	10^{-6}	10^6

Pre-screening on agar plates is an inexpensive method that can sort 10^5 mutants. It requires cell transformation, which is followed by growing those cells in a selective medium [17]. Only cells that contain advantageous proteins survive. However, this method is very limited.

Nowadays, the most used method for library screening is 96-well microtitre plate. To ensure the presence of only one variant in each well it is necessary to inoculate single cells into wells. Subsequently, the substrate is added to wells and the analysis

is performed in a UV-Vis reader, where the absorbance or fluorescence is detected. Using this method, it is possible to screen 10^4 variants [17]. The improvement of the throughput of this method lies mainly in the use of sophisticated and expensive robotic stations instead of picking by hand, which enable the use of bigger microtitre plates with up to 1 536 wells. However, the bigger number of wells, the smaller the volume of them.

Those methods are considered as medium or high throughput screening that defines the ability to perform 10^4 - 10^6 tests per day [31]. The need for miniaturization and increased throughput led to the development of assays and instrumentation for the fast selection of desired proteins. Specifically, fluorescence-activated cell sorting (FACS) is based on the detection of fluoresce in continuous phase in a flow cytometer, which has few limitations due to the absence of compartmentalization [5]. To overcome that, fluoresce-activated droplet sorting (FADS) has been developed enabling the analysis of single droplets in a microfluidic chip. Both FACS and FADS, along with other protein selection techniques, have revolutionized the field of protein engineering and expanded our understanding of protein structure and function.

3.2 Fluorescence-activated droplet sorting systems

In FADS, each droplet can be considered as a separate microreactor. This method is recognized as an ultra-high throughput method because it can perform droplet generation at 30 kHz rates and sorting usually at 2–3 kHz [27]. The volume of reagents is even more reduced to nanoliters (10^{-9} L) or even picoliters (10^{-12} L) per droplet.

Since incubation with the substrate may take place in a closed glass vial it could be considered as closed system in contrary to conventional methods, so it posses minor health risks to lab workers. Substrates for HLDs are halogenated derivates of carbohydrates and are considered to be carcinogens. In open systems, such as microtitre plates, they tend to evaporate which leads to measurement inaccuracies and increases exposure to dangerous chemicals. On the contrary, while performing FADS, the system is closed so the liquid transfers only in the tubing and chip, and the activity measurement takes place inside the chip.

3.3 Lab-on-chip technology

Lab-on-chip concept has brought a major change in the biochemical field because it is expected to be able to perform all steps in the laboratory that include preparation, incubation, pre-treatment, analysis and collection.

The main focus of this thesis is to study the sorting of enzymes haloalkane dehalogenases. LOC represents a better option than conventional methods, because it has a short dead time, requires small reaction volumes, reaches temperature equilibrium in the order of milliseconds and operates at high throughput.

The advantage of the microfluidic field is an individual approach to the application. Therefore even chips differ with respect to the task requirements.

Since the microfluidic system operates on very small dimensions, it is crucial to ensure cleanliness and prevent dust and other impurities from clogging the chip channels.

Besides that, one of the interesting applications of the lab-on-chip are organs-on-chip, which carries all the crucial functions of the living organ. The measurements on such devices enable scientists to explore the impact on organ function to study tissue engineering or the etiology of diseases [6].

3.3.1 Soft lithography and chip fabrication

Soft lithography is used for the fabrication of poly-dimethyl siloxane (PDMS), which is biocompatible, transparent and also cheap.

The process includes designing a mask concerning the application, and the creation of the wafer that is used as a mold for PDMS casting. The subsequent connection with the glass surface enables the formation of channels. The workflow of chip fabrication since creating the wafer mold to functional microfluidic chip with description is depicted in Fig. 3.1.

Emulsion created in chips can be either water-in-oil (W/O) or oil-in-water (O/W) type. One of the compounds is a dispersed phase in a continuous phase [1]. Depending on the type of emulsion, channels must be hydrophobically or hydrophilically modified.

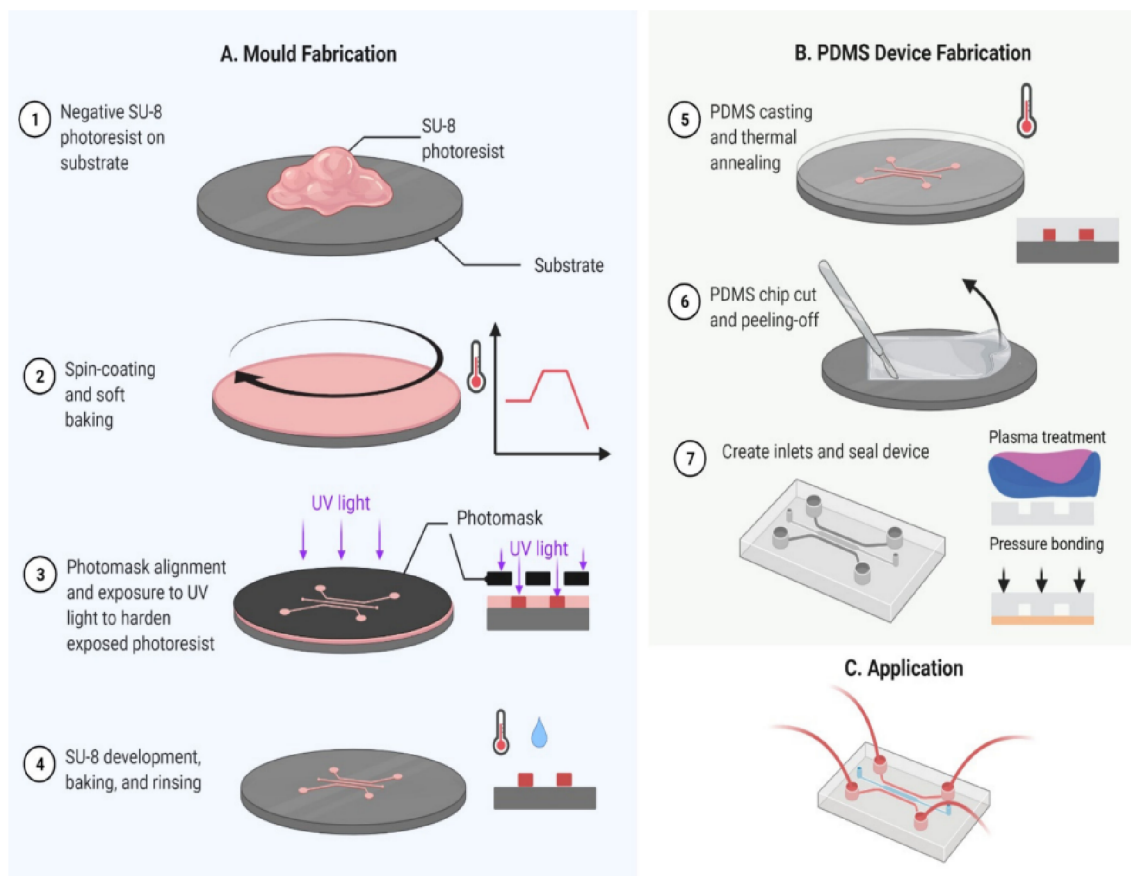


Fig. 3.1: Workflow of microfluidic chip fabrication [24].

3.3.2 Microfluidic chip for droplet generation

Droplet generation, or encapsulation, is a process of creating single or double emulsion droplets. Due to the precision of control, it is possible to generate droplets of the same sizes. For single water-in-oil emulsions 2 phases are present: aqueous and oil phases.

The aqueous phase consists of a detection assay, which is a mixture of cells, fluorescence dye and other substances that are necessary for further screening. It is dispersed into the oil. The flow rate of this phase is several times slower than the oil phase. The encapsulation takes around 1 hour.

The oil phase consists of oil and biocompatible surfactant. Surfactants stabilize the newly formed droplets and prevent them from merging. Droplets generated in this way are stable for days to weeks. Due to the evaporation of fluorinated oil, it is necessary to overlay generated droplets with mineral oil.

The flow in microfluidic devices is in the vast majority of laminar and the mixing of reagents is done by molecular diffusion, which takes seconds in such small dimensions [25].

3.3.3 Surface modification

Even though the PDMS is naturally hydrophobic, the plasma treatment worsens this feature. To enhance the hydrophobicity for water-in-oil emulsions, channels need to be modified with a biocompatible hydrophobic reagent. One of the polymers used for modification is 1 % Trichloro(1*H*,1*H*,2*H*,2*H*-perfluorooctyl)silane in HFE 7500 or FC 40 fluorinated oil that creates a self-assembled monolayer that is superhydrophobic. The residual silane must be washed with oil to avoid clogging the chip [4]. Subsequently, it has to be blow-dried.

3.3.4 Microfluidic chip for droplet sorting

Chip for droplet generation and sorting chip may come in one piece, according to the time necessary for incubation. In the case of a long incubation time, this step takes place outside the chip in the vial.

The sorting chip consists of inlets for droplet re-injection and spacing oil, 2 outlets, and electrodes. Spacing oil is used to increase the gaps between droplets for optimal fluorescence sensing and better control of dielectrophoretic separation. The composition of this oil phase is the same as for droplet generation. 2 outlets are used to separate cells of desired activity and waste. The electrodes apply voltage to the chip and thus enable deviation of the droplet path in case of exceeding the fluorescence limit above the set limit.

The phenomenon that occurs is called dielectrophoresis, depicted in Fig. 3.2.

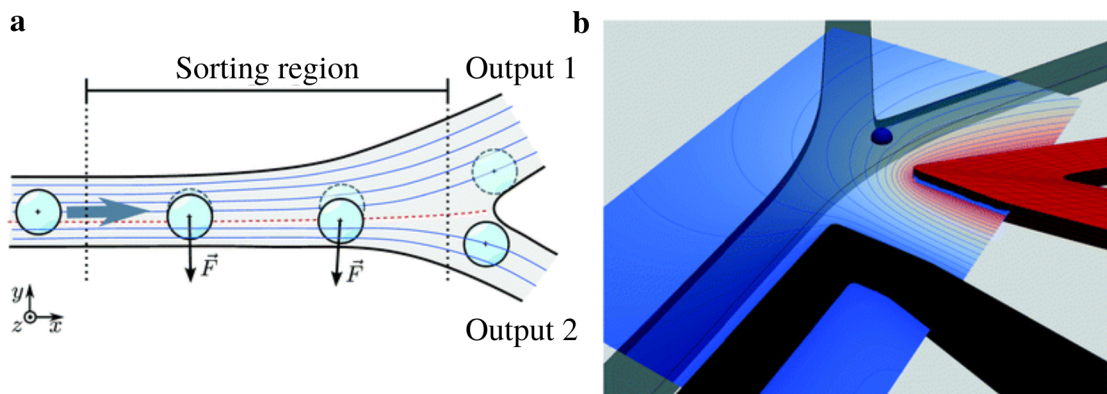


Fig. 3.2: Schematic representation of dielectrophoretic sorting on a chip [23];
a - the dielectrophoresis force changes the trajectory of the droplet into the different channel;
b - visualization of electric field on sorting chip.

The non-uniform electric field is applied on a droplet via electrodes and it results in an induced effective dipole moment of the particle. Force on a dipole depends on the non-uniform electric field. Induced dipoles occur when a particle undergoes polarization. Charges inside the droplet move in opposite directions and form an induced dipole. The dielectrophoretic force causes droplet flow to be deflected depending on their properties [23].

3.4 Technical assembly for droplet sorting

The technical assembly of microfluidic droplet sorters in different labs varies a little.

In 2013 the U.S.A. The National Institute of Health published an article [20] in which they described the protocol of high-throughput analysis and sorting. The setup consisted of a laser as a source of coherent light for excitation with wavelength according to the absorption and emission spectra of fluorescence dye. Several lenses with different focal lengths were inserted into the laser path to focus the laser beam image plane of the microscope objective in an inverted microscope. Besides the laser light, the light source was also present to allow tracking of the trajectories of droplets. As the droplets passed the part of the sorting chip, where the laser was focused, the fluorescence of droplets could be observed. On the side port of the microscope, there were three photomultipliers (PMT) present to detect different emitted colors. Dichroic mirrors with different transmittance and reflection of wavelengths were placed before PMTs and the parasitical lightning was removed by bandpass filters. 80 % of light is routed to the PMTs and the remaining 20 % is routed to the eyepieces. Sorting pulses were amplified by a high-voltage amplifier.

Field Programmable Gate Arrays (FPGA) from National Instruments was used to run custom LabView software that controls the sorting process.

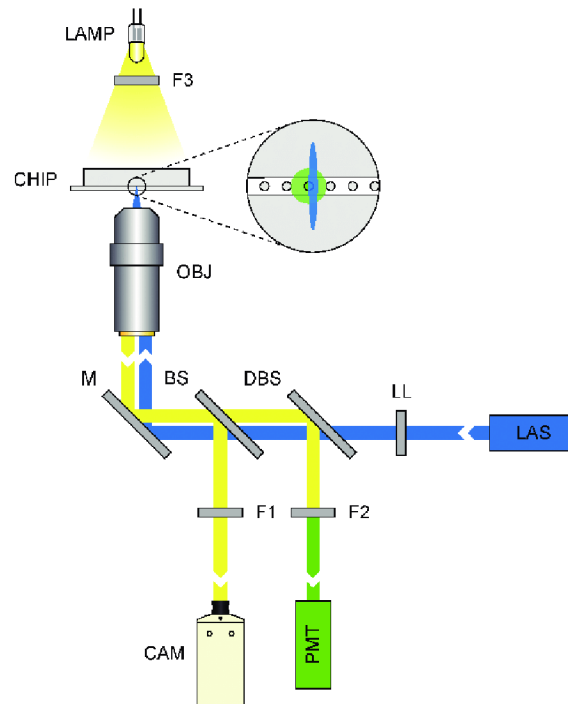


Fig. 3.3: Schematic representation of optical setup with one PMT [5].

Another scientific group from France used a very similar setup for sorting different mutants of enzymes galactosidases [5], which is depicted in Fig. 3.3. However, they only used one PMT to detect only one color. To allow video acquisition and control of the trajectories of droplets on screen the high-speed camera was added to the side of the inverted microscope.

4 Experimental part

The experimental part was focused on the assembly of the sorting system with respect to the application. The list of used components is in Tab. 4.1.

As the system was newly built, the optimization of the fabrication of chips, encapsulation and sorting parameters was also performed. After the description of the system, the cultivation process and sorting experiment were discussed. The list of used chemicals with a description is in Tab. 4.2.

The final part contains software for analyzing the obtained data in .tdms format, which was implemented in the LabView environment bundled with Python function.

Tab. 4.1: List of components used in construction of Fluroescence Activated Droplet Sorting system.

Name of component	Company	Country
Automatic pumps neMesys	Cetoni	Germany
CELESTA Light Engine	Lumencor	USA
Gastight glass syringes	Hamilton	USA
High-speed camera i-SPEED TR	Olympus	Japan
High-voltage amplifier TREK 2210	TREK	USA
Infinity 2 fluorescence camera	Teledyne Lumenera	Canada
Inverted microscope IX73	Olympus	Japan
Motorized scanning stage	Märzhäuser Wetzlar	Germany
M660L4 LED light source	Thorlabs	Germany
NI FPGA R Series 7842	National Instruments	USA
Optical cage with lenses and mirrors	Thorlabs	USA
Oscilloscope DSOX1204	Keysight	USA
Photomultiplier H10723-20	Hamamatsu	Japan
Pressure controller OB1	Elveflow	France
Shielded I/O connector SCB-68A	National Instruments	USA

Tab. 4.2: List of used chemicals.

Name of chemical	Company	Country
Aminophenyl fluorescein	Sigma-Aldrich	USA
Anhydrotetracycline	Cayman Chemical	USA
1,2-Dibromomethane	Sigma-Aldrich	USA
1 % (w/w) 008-FluoroSurfactant	RAN Biotechnologies	USA
HFE 7500	3M	USA
Hydrogen peroxide	Penta Chemicals	Czech Republic
8-Hydroxypyrene-1,3,6-trisulfonic acid trisodium salt	Sigma-Aldrich	USA
Luria-Bertani medium	Sigma-Aldrich	USA
Mineral oil	Sigma-Aldrich	USA
OptiPrep™ Density Gradient Medium	Sigma-Aldrich	USA
(1 <i>H</i> ,1 <i>H</i> ,2 <i>H</i> ,2 <i>H</i> -perfluorooctyl)silane	Sigma-Aldrich	USA
Potassium phosphate monobasic	Lach:ner	Czech Republic
Potassium hydrogen phosphate	Lach:ner	Czech Republic
Sodium Orthovanadate	Sigma-Aldrich	USA
184 Silicone Elastomer base	Sylgard	USA
184 Silicone elastomer curing agent	Sylgard	USA
Super optimal broth with catabolite repression	New England BioLabs	USA
Trichloro(1 <i>H</i> ,1 <i>H</i> ,2 <i>H</i> ,2 <i>H</i> -perfluorooctyl)silane	Sigma-Aldrich	USA
Vanadium-dependent chloroperoxidase	in-house made	Czech Republic

4.1 Fluorescence-activated droplet sorting system

The Loschmidt Laboratories cooperate with colleagues from Eidgenössische Technische Hochschule (ETH) in Zürich (Eng. Swiss Federal Institute of Technology) on many microfluidic applications. The assembly depicted in

Fig. 4.1 and Fig. 4.2, was inspired by assembles from literature and by the set used at ETH. The list of components is in Tab. 4.1. This part of the thesis was focused on the optimization of the setup.

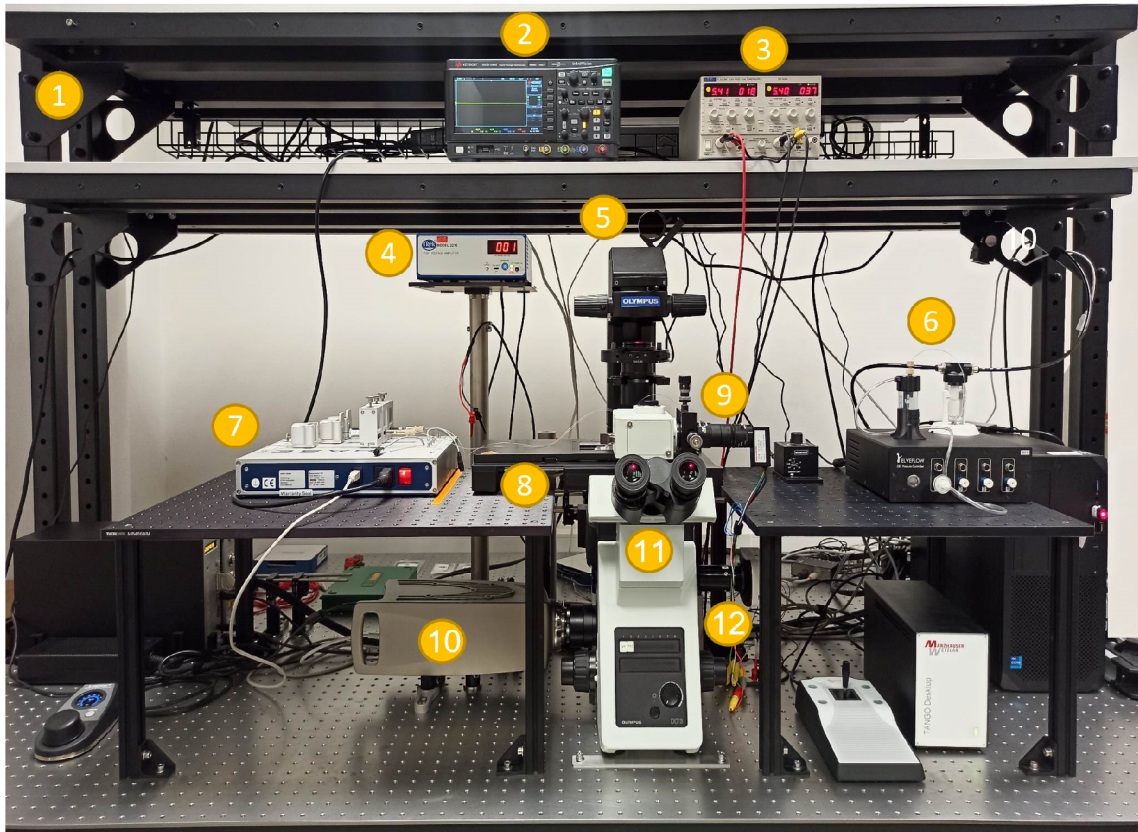


Fig. 4.1: Newly assembled setup used for droplet sorting - front view;

1	Optical Table	5	LED light source	9	Photomultiplier
2	Oscilloscope	6	Pressure pumps	10	High-speed camera
3	Voltage generator	7	Automatic pumps	11	Inverted microscope
4	High-voltage amplifier	8	Motorized stage	12	Fluorescence camera

The whole system was placed on the optical table with an active insulator leg bundles. It eliminated vibrations, which was important mostly for the sorting part of the experiment.

CELESTA Light engine was used as a laser radiation source with a cyan laser with a wavelength of 477 nm for excitation. Laser beam passed through the objective, iris and lenses to the microscope.

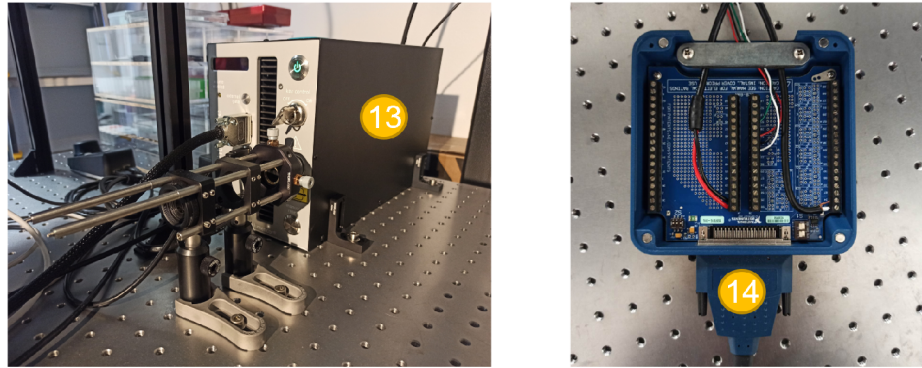


Fig. 4.2: Newly assembled setup used for droplet sorting - back view;

13 CELESTA Light Engine 14 Acquisition Card

Next, the laser beam was reflected from the visible light mirror to the telescope part that focused the light beam into a single point on the specimen on the microscope stage. The telescope part was composed of another visible light mirror that reflected the light to plano-convex lens with a focal length of 30 mm with a convex side oriented to a laser and another plano-convex lens oriented the other way. The light beam then passed through a mounted plano-convex lens with a focal length of 300 mm. Subsequently, it was reflected on the right-angle dichroic mirror in the carousel and directed to the specimen (channel) through the microscope objective. Initial experiments aimed to focus the laser on the chip to achieve the highest signal on the photomultiplier (PMT).

The core of the FADS system consisted of an inverted microscope used for placing the chip, checking the cleanness of chips, droplet generation, and sorting. It played a crucial role in laser focusing as well. The fluorescence filters cube turret, underneath the nosepiece, was equipped with the fluorescence cube containing a dichroic mirror suitable for Fluorescein isothiocyanate (FITC) and 8-hydroxy-1,3,6-pyrenetrisulfonic acid trisodium salt (HPTS) as well. From the objective carousel, the microscope semiapochromat objective with 10 \times or 20 \times magnification with a long working distance was used. Transmitted light could be split between cameras or a PMT attached to the microscope. Microfluidic chips were placed on the motorized scanning stage.

The high-speed camera enabled monitoring of the experiments on the microfluidic chips at a high framerate – up to 10 000 fps. For tracking the fluorescence, the fluorescence camera was attached to the microscope. This camera was also used for laser focusing. Photomultiplier was mounted on the trinocular tube and was used for the detection of low-level fluorescence emission. PMT was connected to the Shielded I/O connector terminal block interfacing analog and digital signals to the FPGA. Sorting software and the FPGA were programmed using LabVIEW and

LabVIEW FPGA module. There, the user chose the sorting parameters that decided whether the voltage value fitted the sorting threshold. If so, the FPGA card sent sorting pulses (1–10 V) to a high-voltage amplifier that amplified the signal 100 times and generated the series (typically 20–60) of dielectrophoretic pulses on the chip. The shape and correct course of pulses was graphically displayed on the oscilloscope.

Apart from the optical setup, the pumps for the injection of cells, oils, and the reinjection of droplets were installed. The automatic syringe pumps enabled precise control of flow rates of phases. Glass syringes were used in each experiment for higher reproducibility of generated droplets. The pressure and flow controller with compressor allowed droplet reinjection on the sorting chip using pressurized air applied on the in-house made reservoir containing the droplets.

4.2 Fabrication of microfluidic chips

Chips for droplet encapsulation and fluorescence-activated droplet sorting were fabricated using Polydimethylsiloxane (PDMS) elastomer due to its price and suitable properties such as biocompatibility. Fabrication was done according to the protocol well established in Loschmidt laboratories.

The silicone elastomer base was mixed with a crosslinker in a ratio of 10:1. Both components were intensively mixed for 3 minutes. To avoid bubbles that could damage the channels of the microfluidic chip, the PDMS needed to be degassed in a desiccator with a vacuum till no bubbles were present. The degassed mixture was then poured on a wafer attached to a plastic dish. Subsequently, the chip was baked at 65 °C for at least 3 hours using the universal oven UF30 (Mettler, Germany).

When the chip solidified in the oven, it was cooled down to room temperature. PDMS chips were then cut, concerning the design on a wafer, and peeled off. Holes for inlets, outlets and electrodes were created with the use of Ø1 mm UniCore Punches (QUIAGEN, Germany). The chips were bonded to glass slides. Plasma treatment (Plasma Etch PE-75, USA) was set to plasma time of 5 minutes, the vacuum of 200 mtorr, 30 seconds ventilation time and emergency ventilation of 10 seconds, according to the application. Bonded chips were cured on Hot Plate at 80 °C for 20 minutes and covered with scotch tape to avoid dust.

4.2.1 Optimization of droplet quality

The stability of the droplets is based on the quality of the silanization, concentrations of surfactant in the oil phase, the purity of the used tubing and vials as well as prevention of evaporation.

The hydrophobic modification was performed after the fabrication of the chip. Different parameters were combined and tested. Combinations used for optimization regarding the composition of the oil phase are in Tab. 4.3.

Tab. 4.3: Combinations of oil and surfactant of different concentration used for oil phase optimization.

Oil	Surfactant	Concentration
FC 40	Fluosurf	0.5 %
FC 40	Fluosurf	1 %
FC 40	Fluosurf	2.5 %
FC 40	Fluosurf	5 %
HFE 7500	RAN	0.5 %
HFE 7500	RAN	1 %
HFE 7500	RAN	2.5 %
HFE 7500	RAN	5 %

Different oil phases were used to generate droplets in microfluidic chips that were modified using several procedures described in Tab. 4.4. FC 40 oil was the oil of the first choice due to the better parameters regarding the substrate incubation, because it was better in terms of the transfer of the substrate from oil to a droplet. Additionally, another widely used oil HFE 7500 was also added to the optimization process. Alternatively, propanol and acetic acid were used as solvents for surfactant.

Corresponding concentration of the silanizing agent in oil, either Trichloro(1*H*,1*H*,2*H*,2*H*-perfluorooctyl)silane (TCPS) or alternatively (1*H*,1*H*,2*H*,2*H*-perfluorooctyl)silane (FOTS) were prepared to create self-assembled monolayer on PDMS.

Glass vials, that were used for collecting generated droplets and for incubation were modified with TCPS in toluene, according to the protocol published in *Angewandte Chemie* [9]. Silanization consisted of plasma treatment, incubation with TCPS diluted in toluene, sonication and washing. Vials were then dried and used for collection

Tab. 4.4: Combinations used for optimising surface modification process.

Spincoat	Silane	Concentration	Solvent	Incubation	Temperature
Yes	FOTS	1 %	FC 40	5 minutes	25 °C and 80 °C
Yes	FOTS	3 %	FC 40	5 minutes	25 °C and 80 °C
Yes	FOTS	5 %	FC 40	5 minutes	25 °C and 80 °C
No	FOTS	1 %	FC 40	5 minutes	25 °C and 80 °C
No	FOTS	3 %	FC 40	5 minutes	25 °C and 80 °C
No	FOTS	5 %	FC 40	5 minutes	25 °C and 80 °C
No	TCPS	1 %	FC 40	2 hours	25 °C and 80 °C
No	TCPS	3 %	FC 40	2 hours	25 °C and 80 °C
No	TCPS	5 %	FC 40	2 hours	25 °C and 80 °C
Yes	FOTS	1 %	HFE 7500	5 minutes	25 °C and 80 °C
Yes	TCPS	1 %	HFE 7500	5 minutes	25 °C and 80 °C
Yes	FOTS	3 %	HFE 7500	5 minutes	25 °C and 80 °C
Yes	TCPS	3 %	HFE 7500	5 minutes	25 °C and 80 °C
Yes	FOTS	5 %	HFE 7500	5 minutes	25 °C and 80 °C
Yes	TCPS	5 %	HFE 7500	5 minutes	25 °C and 80 °C
No	FOTS	1 %	HFE 7500	2 hours	25 °C and 80 °C
No	TCPS	1 %	HFE 7500	2 hours	25 °C and 80 °C
No	FOTS	3 %	HFE 7500	2 hours	25 °C and 80 °C
No	TCPS	3 %	HFE 7500	2 hours	25 °C and 80 °C
No	FOTS	5 %	HFE 7500	2 hours	25 °C and 80 °C
No	TCPS	5 %	HFE 7500	2 hours	25 °C and 80 °C
No	TCPS	1 %	Propanol	5 minutes	25 °C and 80 °C
No	TCPS	5 %	Propanol	5 minutes	25 °C and 80 °C
No	TCPS	1 %	Propanol	2 hours	25 °C and 80 °C
No	TCPS	5 %	Propanol	2 hours	25 °C and 80 °C
No	TCPS	1 %	Acetic Acid	10 minutes	25 °C and 80 °C

4.2.2 Encapsulation chip

The encapsulation chip, shown in Fig. 4.3, has 2 inlets and 1 outlet. This type of design is called flow-focusing microdroplet generator.

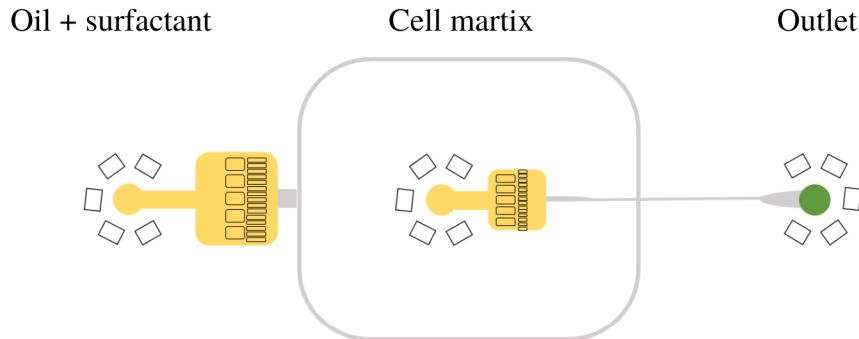


Fig. 4.3: Design of the encapsulation chip.

One of the inlets was used for the oil phase, in this case for a solution of 1 % (w/w) 008-FluoroSurfactant RAN surfactant in HFE 7500 oil. Surfactant is a substance that reduces surface tension, and it should prevent droplets from merging. HFE 7500 oil is fluorinated oil that is colorless and biocompatible. It was suitable for water-in-oil emulsions, that were used in this thesis.

The second inlet was used for the aqueous phase that consisted of the 8-Hydroxypyrene-1,3,6-trisulfonic acid trisodium salt (HPTS) solution in buffer or library produced in cells. Generated droplets were collected from the outlet directly into a modified conical glass vial.

Although PDMS material was naturally hydrophobic, the plasma treatment reduced its hydrophobicity. Therefore, additional surface modification was performed.

Bonded PDMS chip was modified with a hydrophobic silane solution that consisted of 1 % TCPS in filtrated HFE 7500. The chip was ready to use immediately and described modification can last up to several months.

4.2.3 Sorting chip

The sorting chip was designed at ETH Zürich in the deMello group. The design is shown in Fig. 4.4. Since the single W/O emulsion is already stabilized by fluorosurfactant and surrounded by oil, it was not necessary to modify the surface of the sorting chips.

Electrodes are major components of sorting microfluidic chips. Field's metal was used for the fabrication of them. It is a eutectic alloy that consists of 32.5 % bismuth, 51 % indium and 16.5 % tin [32]. It has suitable properties, such as conductivity,

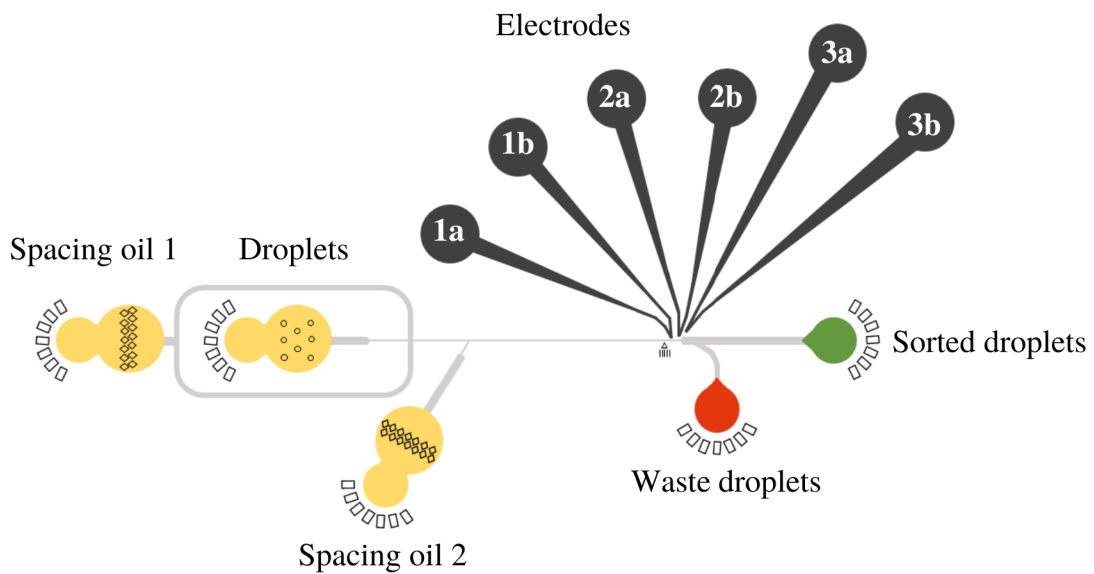


Fig. 4.4: Design of the sorting chip.

lower toxicity than other alternatives (e.g. Woods metal) and a melting temperature of around 62 °C. To manufacture wires, metal granules were melted in an aluminum dish on Hot Plate set to 100 °C. A syringe and Teflon tube (Ø1 mm) with the oblique cut at one end was used for pulling melted metal. After cooling, the tubing was carefully removed, and newly created wires were cut into pieces that fit into PDMS sorting chip.

Pieces of Field’s metal wires were inserted into inlets marked with 1a, 2a and 3a in Fig. 4.4. Copper wires (Ø1.5 mm) with a length of 5 cm with removed insulation from both sides were inserted into holes marked with 1b, 2b and 3b. The whole chip was put onto Hot Plate set to 100 °C until electrode channels filled up with metal. After proper melting, the chip was removed from Hot Plate and cooled down to room temperature.

The microscope and multimeter were used for checking the correct filling of channels, and thus whether all of them were separate and not interrupted by measuring the resistance of neighboring holes for electrodes: 1a with 1b, 2a with 2b and 3a with 3b.

4.3 Optimization of droplet sorting system

As the system was newly assembled, it was important to align the laser into the optical path and focus the beam into a microfluidic channel. From the point of view of cell encapsulation and fluorescence detection, the flowrates of all liquids and

reinjecting droplets were optimized.

4.3.1 Encapsulation

The necessary equipment needed for encapsulation is in the list below:

- 1 ml glass syringe for the oil phase
- 250 μL glass syringe for the reaction mixture
- Hydrophobically modified encapsulation chip
- Teflon tubing with an outer diameter of 1 mm
- Hydrophobically modified conical glass vial
- 3D printed vial holder

The tubing was connected to the syringes and the free end of the tubing was inserted into the corresponding inlet. After the first few experiments, it was observed, that the droplets tend to gelatinize if exposed to air and moreover they did not have a uniform size. To avoid this, a modified glass vial was pre-filled with 400 μL mineral oil.

The short tubing pre-filled with mineral oil was inserted into the outlet of the encapsulation chip. The pumps were set to corresponding syringes and flow rates were set to the size of encapsulated cells. Encapsulation parameters are in Tab. 4.5.

Tab. 4.5: Encapsulation parameters - flowrate settings

Fluid	Flowrate
Oil phase	300 $\mu\text{L}/\text{hour}$
Aqueous phase	80 $\mu\text{L}/\text{hour}$

4.3.2 Sorting

Sorting and screening was the next step after the droplet generation.

The equipment consisted of:

- 250 μL glass syringes for oil phase 2 \times
- Sorting chip
- Tubing with an outer diameter of 0.85 mm
- Glass vials for sorted and waste droplets 2 \times
- In-house made reservoir containing the droplets

The inlet part of the falcon tube was designed with Autodesk Inventor. Bottom holder was made by ESSI tech and the cap for tubing and pressure was made by

Elveflow. The reservoir with the design of a Falcon tube inlet used for sorting is depicted in Fig. 4.5.



Fig. 4.5: In-house made reservoir for droplet reinjection;
a - PC model of vial holder;
b - Reservoir assembly used in the lab.

The two inlets for the oil phase were used for the spacing of the droplets. The flowrate of the droplets was decreased in order to ensure precise analysis and proper sorting. Spacing oil 2 was tested for higher flowrates so the flow of droplets was directed to the waste channel and only those with the selected activity were attracted to the sorted outlet. This parameter helped to reduce the false positive hits. The resulting sorting parameters are in Tab. 4.6.

Tab. 4.6: Sorting parameters - flowrate settings.

Parameter	Flowrate/Pressure
Spacing oil 1	10 $\mu\text{L}/\text{hour}$
Spacing oil 2	15 $\mu\text{L}/\text{hour}$
Pressure of droplet reinjection	65 mBar

4.3.3 Laser focusing with fluorescent dye

The laser was focused with the use of a fluorescence camera, PMT and sorting software. It was important to obtain the highest signal that was analyzed during the sorting.

For the experiment, the HPTS with the concentrations of 10 $\mu\text{mol}/\text{L}$, 40 $\mu\text{mol}/\text{L}$ and 70 $\mu\text{mol}/\text{L}$ in 20 mmol/L phosphate buffer with a pH of 8.2 were encapsulated in an encapsulation chip. HPTS is a fluorescent pH indicator with an excitation

peak of 460 nm and an emission maximum of 510 nm, which is very similar to the APF.

The first step was the encapsulation of all concentrations separately. The aqueous phase consisted of the HPTS solution with the corresponding concentration and the oil phase consisted of 1 % surfactant in HFE 7500 oil. The flowrate of the oil phase was 300 $\mu\text{L}/\text{hour}$ and for the aqueous phase 80 $\mu\text{L}/\text{hour}$.

The initial laser focusing was performed in the inlet of the encapsulation chip because the fluorescence intensity there is the highest and continuous as the droplets are not formed yet. Moreover, it enabled better precision in controlling the shape of a laser.

The focusing could be affected by adjusting lenses and mirrors in the optical path for the laser, focusing of the microscopy objective and positioning the microfluidic chip using the motorized stage. Emission light was focused on the detector by XY translator. After obtaining the highest signal, the position of the chip was moved behind the T-junction to track the movement of the droplets. The focus was then adjusted just a little. The droplets of all concentrations were encapsulated for 1 hour each, to have all fluorescence intensities evenly represented.

The next step was the sorting of the droplet mixture. It was performed according to the sorting parameters described in Tab. 4.6. The laser was focused into the channel to a specific point and the intensities were measured. That was the last step for proper focusing to obtain the highest signal for the actual protein sorting that was performed as the next step.

After measuring, this experiment was considered as the first benchmark experiment so the other sorting experiments could be done.

4.4 Sorting experiment

4.4.1 Protein production

Production of desired protein was a crucial step for further experiments. Commercial chemically competent *Escherichia coli* (*E. coli*) BL21(DE3) cells were used for Heat shock transformation. Cell transformation allows the addition of the plasmid with a gene encoding desired protein into cells.

For the benchmark experiment, which was performed to evaluate the sorting quality of the newly assembled sorter, three different plasmids for cell transformation were used. As a negative control, the empty pIDR9 plasmid, which carried no gene, was produced. To be able to evaluate higher fluorescent intensities, DhaA31 and ancHLD-RLuc were produced as well. The final mixture

consisted of 5 % of DhaA31, 45 % of ancHLD-RLuc and 50 % of empty pIDR9, mimicking the intensity distribution in the library.

After the benchmark, the InDel library was produced for sorting experiment with corresponding plasmids.

The transformation started by mixing 10 μ L of cell suspension with 1 μ L of plasmids (to reach the concentration of 100 ng/ μ L). Cells were left on ice for 30 minutes and then the Heat Shock was induced by putting the mixture into Thermoblock (Eppendorf, Germany) at 42 °C for 30 seconds. In this stage, the cell membrane became more permeable and added plasmids could transfer into cells. Cells were then incubated on ice for 5 minutes. Subsequently, 200 μ L of SOC medium (a variant of Super Optimal Broth with catabolite repression) was added to provide nutrients and allowed recovery and stabilization of cells after transformation. Cells were incubated at 37 °C for 70 minutes while shaking on Incubation Orbital Shaker at 180 rpm.

After incubation, cells were moved into bigger volumes with 10 ml of LB medium (Lauria-Bertani medium) inoculated with 10 μ L of ampicillin for all expressed variants to allow the selection of only desired cells. The culture was incubated overnight.

The next day, pre-culture was diluted with LB broth and incubated for 1 hour at 37 °C and shaken at 180 rpm. After reaching $OD_{600}^1 = 0.4-0.6$, anhydrotetracycline was used to induce the gene production which took 5-7 hours at 20 °C.

Cells were harvested by centrifugation at 4 °C and 4000 rcf for 15 minutes. It allowed cells to separate from LB broth. The supernatant, the fluid above sediment mostly consisting of LB broth was discarded and the pellet, the remaining cells, was resuspended in 20 mmol/L Phosphate Buffer with 1 mmol/L Na_3VO_4 . Centrifugation was repeated 1 more time and cell density was adjusted to reach the final value $OD_{600} = 10$.

4.4.2 Reaction mixture

Halide oxidation assay (HOX) for halide detection consisted of [3]:

- 50 μ L OptiPrep™
- 20 μ L vanadium-dependent chloroperoxidase (300 international units)
- 2 μ L 100 mmol/L H_2O_2
- 0.8 μ L APF (5 mmol/L in dimethylformamide)
- 0.85 μ L *E. coli* cells with produced protein, $OD=10$
- 126 μ L 20 mmol/L Phosphate buffer, pH = 8.2

¹ OD_{600} is the spectrophotometer method to estimate the concentration of bacteria in a medium measured at 600 nm wavelength. $OD_{600}=1$ refers to the concentration of $5 \cdot 10^8$ cells/ml of *E. coli*.

OptiPrep was used for the stabilization of the suspension, because it prevented sedimentation of the cells in the syringe during droplet generation. Normally, cells would sediment, but OptiPrep allowed cells to isolate and enabled problem-free reinjection of cells to the sorting chip. VCPO enzymes oxidize halogens into the corresponding hypohalous acids. APF is a fluorescent probe, that is converted by hypohalous acid into fluorescein that could be detected.

The amount of 0.85 μL produced cells were added to filtrated HOX assay mixture. The encapsulation was performed under the conditions mentioned in Tab. 4.5. Droplets with encapsulated cells were collected into a conical vial filled with mineral oil. Encapsulation took from one to two hours and approximately 30 million droplets were generated.

The residual oil phase on the bottom of the vial (phases are depicted in Fig. 5.5) was removed with a syringe. 100 μL of 1,2-Dibromoethane (DBE) in the same solution as the oil phase was added at the top of the mineral oil overlay to reach the concentration of 0.3 mmol/L. The incubation with substrate took 40 minutes. Again, the residual phase at the bottom was removed and droplets were washed with substrate-free oil with surfactant three times. Flowrate/pressure parameters are mentioned in Tab. 4.6.

4.4.3 Software settings of the experiment

After incubation, the conical vial was put into an in-house made pressure chamber reservoir and the outlet of such reservoir was connected to the inlet of the sorting chip. The air inlet of the reservoir was connected to the OB1 pressure controller adjusting the pressure, respectively the flowrate of re-injected droplets.

Signal measuring and the sorting logic were programmed in LabView environment. The parameters of dielectrophoretic pulses and laser used for sorting are in Tab. 4.7.

Tab. 4.7: Sorting parameters.

Parameter	Value
Amplitude	7-9 V
Frequency	30 000 Hz
Burst	30 - 60
Delay	10-40 μs
Laser intensity	75 %

5 Results and discussion

5.1 Droplet quality optimization

Due to the merging of droplets and wetting modification, depicted in Fig. 5.1, the solutions for hydrophobic modification and oil phase needed to be optimized. The picture shows a collection channel after the flow-focusing droplet generator. Ideally, uniform droplets should be observed, however, no droplets were formed and the aqueous phase was wetting.

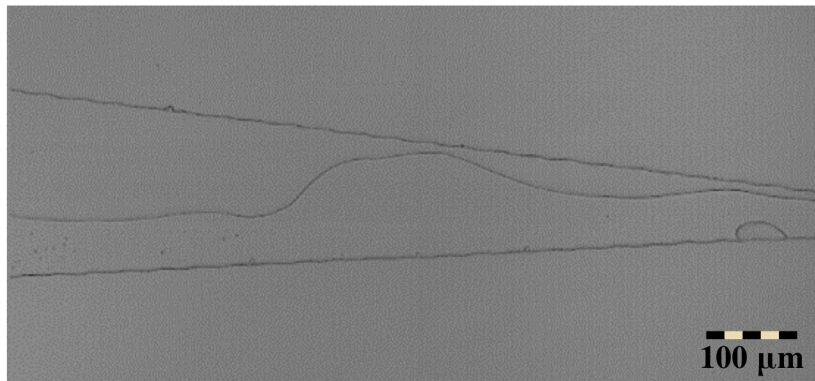


Fig. 5.1: Picture of wetting the channel of the microfluidic chip. In the picture, the incorrect hydrophobic modification is shown. The microfluidic chip was hydrophobically modified with 1 % FOTS in FC 40 oil. Microscope magnification: 10x

The hydrophobic modification was performed for stable and reproducible generation of water-in-oil emulsions. 26 various combinations of parameters given in the Tab. 4.4 were tested on the FADS system.

It was observed that the spin-coated PDMS on the glass slide resulted in impurities in microfluidic channels that caused clogging during encapsulation. It was not possible to reuse clogged chips.

Regarding the modification and droplet generation with fluorinated oil FC 40, the optimal combination of parameters has not been found yet, although this oil is better in terms of the transfer of the substrate from oil to the droplet. One promising combination seemed to be with the spincoated glass with PDMS with 5 % FOTS in FC 40 oil. However, the droplets that formed were too small and the modification lasted only for a few minutes, which is inappropriate for the chosen application. Droplets generated on chip modified with this procedure are in Fig. 5.2

Optimal solutions for modification and oil phase were obtained using HFE 7500 and propanol so far. However, modifications with propanol preserved their good

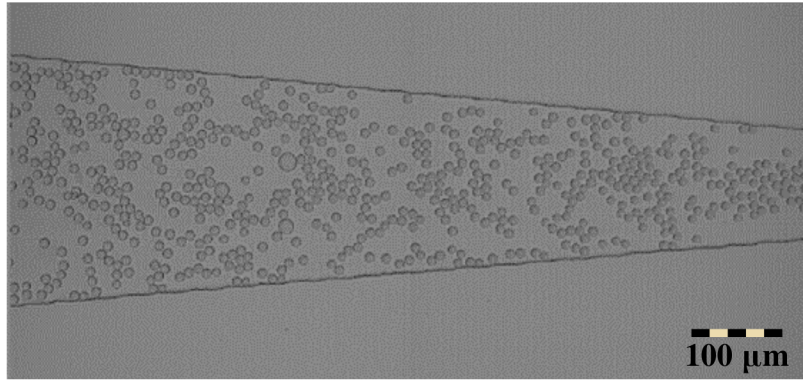


Fig. 5.2: Picture of droplets generated in microfluidic chip hydrophobically modified with 5 % FOTS in FC 40 oil. Microscope magnification: 10x

quality only for a few months, then the generated droplets were not uniform and the chip tended to clog. The best results were achieved by the optimal configuration of parameters described in Tab. 5.1.

Tab. 5.1: Final parameters for hydrophobic modifications.

Spincoated	Oil	Silane	Incubation time
No	HFE 7500	TCPS 1 %	5 min (25 °C)

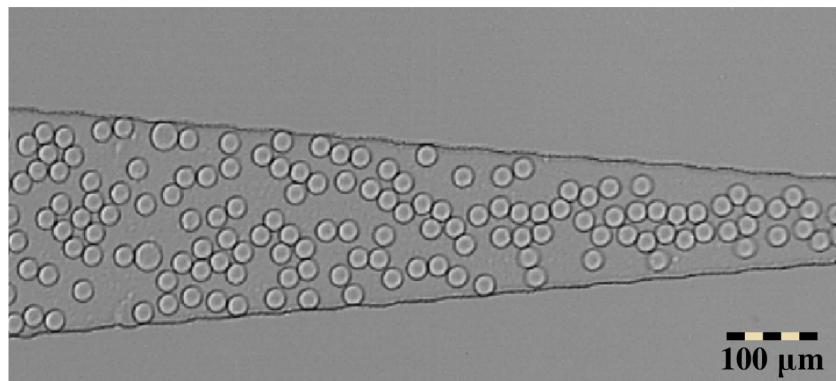


Fig. 5.3: Picture of droplets generated in microfluidic chip hydrophobically modified with 1 % TCPS in HFE 7500 oil. Microscope magnification: 10x

The chosen silanization agent had no impact on the quality of the chip, however, concentrations above 5 % often resulted in clogging. The resulting concentration of 1 % was a compromise between quality and lower chemical consumption. The incubation time of TCPS was set to 5 minutes because longer intervals had no impact on the quality of droplets. Droplets generated according to the procedure described above are depicted in Fig. 5.3 marked with a.

Exposure of droplets to air resulted in gelatinization and it was not possible to continue with reinjection and sorting. This process is depicted in Fig. 5.4. It was most likely caused by the evaporation of the water from droplets. To avoid this process, the mineral oil was used in the collection tubing and collection vial. The amount of mineral oil added to the modified conical vial was set to 400 μL .

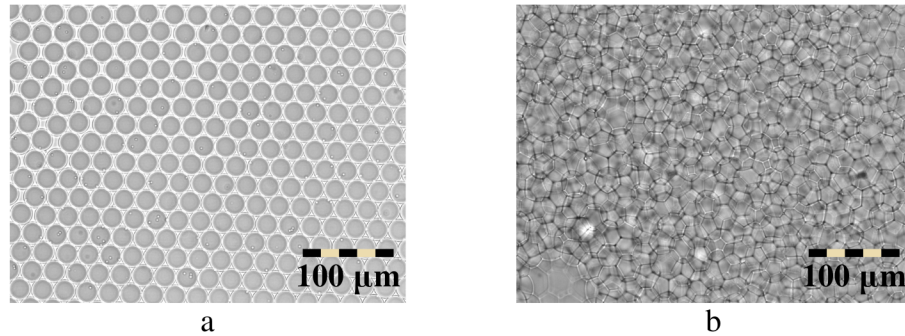


Fig. 5.4: Images from the microscope depicting the process of gelatinization of droplets after exposure to the air, microscope magnification: 20x;
a - droplets that are not merged and gelatinized;
b - gelatinized droplets with modified borders.

In Fig. 5.5, there is depicted glass vial with three layers that formed during encapsulation; mineral oil at the top, a droplet layer in the middle and oil with surfactant at the bottom.

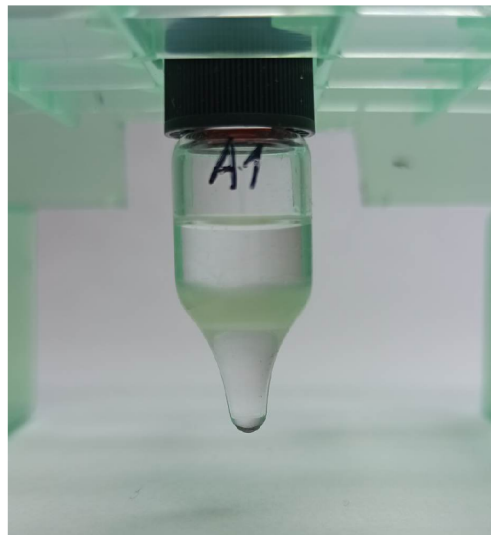


Fig. 5.5: Glass vial with mineral oil on the top, droplets in the middle layer and residual oil with surfactant at the bottom.

This process of hydrophobic modification and oil phase with HFE 7500 led to repeatedly good quality of droplets and lasted several months.

5.2 Optimization of sorting chip fabrication

The channels in the sorting chip have smaller dimensions than the encapsulation chip, both for the fluid channels and electrode channels.

At first, channels for fluid were modified according to the previously optimized modification. This step most likely led to the clogging of the chip. Due to the creation of water-in-oil emulsions that were reinjected into this chip. To avoid clogging, the step for modification was left out. The reinjected droplets did not merge and the flow of droplets was not problematic. By skipping this step it was possible to achieve better purity. Moreover, while pumping the silanization solution into the chip, inlets for electrodes could not be fully covered. It resulted in oil getting into electrode channels, which made it impossible for Field's metal to fulfill the channels, so skipping it led to properly fabricated sorting chips.

To achieve better contact of cables and electrodes, it was necessary to produce thicker chips with a thickness of 6 mm and the diameter of inlet holes corresponding to the diameter of wires.

After those optimization steps, the sorting chips were working properly. The fabricated sorting chip is shown in Fig. 5.6.

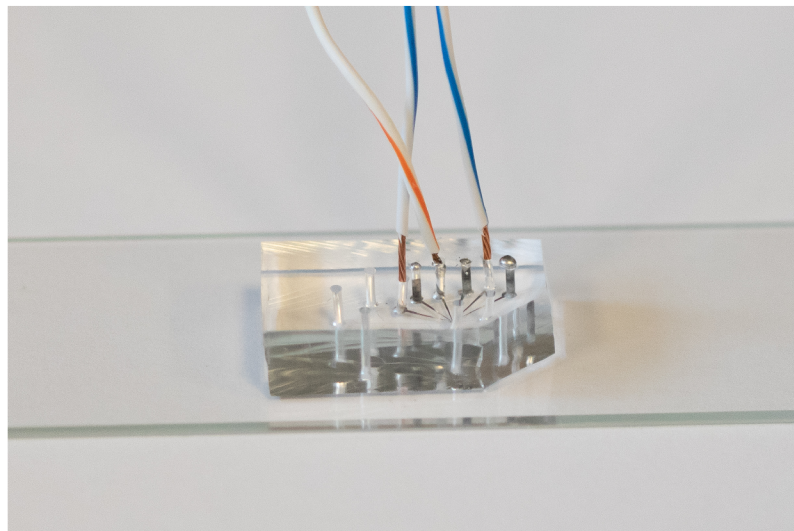


Fig. 5.6: Sorting chip after optimization of the fabrication process.

To test the functionality of the electrodes and pulses, the program was set to sort droplets with high activity. It was possible to control the changes in trajectory in the chip via high-speed camera. Waste droplets continued to the top (waste) channel and droplets with activity over the threshold changes its trajectory into channel close to electrodes, as depicted in Fig. 5.6.

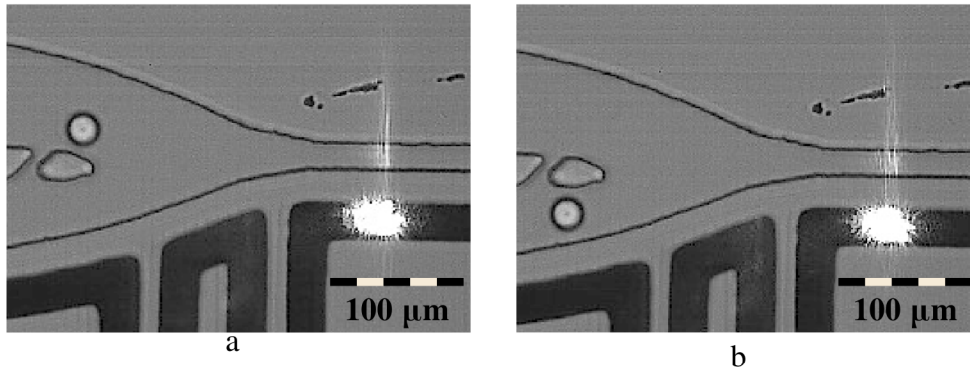


Fig. 5.7: Droplet without and with applied dielectrophoretic pulse, microscope magnification: 20x;

a - waste droplet with low fluorescence;

b - sorted droplet with higher fluorescence.

5.3 Software for data analysis

So far, the basic analysis tools are available in the acquisition software in the LabView environment. This software for sorting was originally developed in Abate Lab at the University of California, San Francisco and is available on GitHub [11]. It has passed through changes in the LL lab and is continuously being modified.

However, those analyzing tools were insufficient, and it required better data analysis, data processing and better visualization of results. For that reason the saving format used in acquisition software was modified and a new application for FADS data analysis was programmed in LabView and Python with the help of the microfluidic team at Loschmidt Laboratories.

5.3.1 New saving format

LabView is a graphical programming language, that enables also the communication and control of FPGA card. The experiment was controlled using the software for sorting in LabView. The software enabled a user to set the detection and sorting parameters, such as the amplitude, frequency and cycles of the pulse or the parameters of a detected peak. Based on the detected intensity and set parameters, the program could decide whether to send the dielectrophoretic pulses via FPGA card onto the chip. Originally, the software enabled a user to save the measurement data in .acq format, in which it is not easily possible to handle with metadata that are necessary for later analysis of the experiment.

Tab. 5.2: List of data stored in TDMS file from the experiment.

Parameter	Unit
Burst cycles	-
Date	-
Description	-
Droplet reinjection pressure	mBar
Encapsulation flow-rate - oil	$\mu\text{L}/\text{hour}$
Encapsulation flow-rate - aqueous phase	$\mu\text{L}/\text{hour}$
Laser intensity	%
Laser wavelength	nm
Name	-
PMT1 gain control voltage	V
PMT2 gain control voltage	V
Pulse amplitude	V
Pulse delay	μs
Pulse frequency	Hz
Sample - aqueous phase	-
Sample - oil phase sample	-
Sampling frequency	Hz
Signal PMT1	V
Signal PMT2	V
Signal sorting pulses	V
Sorting flow-rate - oil 1	$\mu\text{L}/\text{hour}$
Sorting flow-rate - oil 2	$\mu\text{L}/\text{hour}$
Sorting threshold	V
Title	-

For this purpose, the saving format was changed from .acq to binary format .tdms, which is the native format of LabView. The length of 1 TDMS file was set to 2 000 rows. Besides the measurement data, it is containing also metadata, that are important for final data analysis and report from the sorting experiment. A list of saved data and metadata is provided in Tab. 5.2.

5.3.2 Graphical User Interface

The software for analyzing sorting data was implemented in LabView bundled with Python functions. The graphical user interface (GUI) of **Cinderella Analyser** software is illustrated in Fig. 5.8.

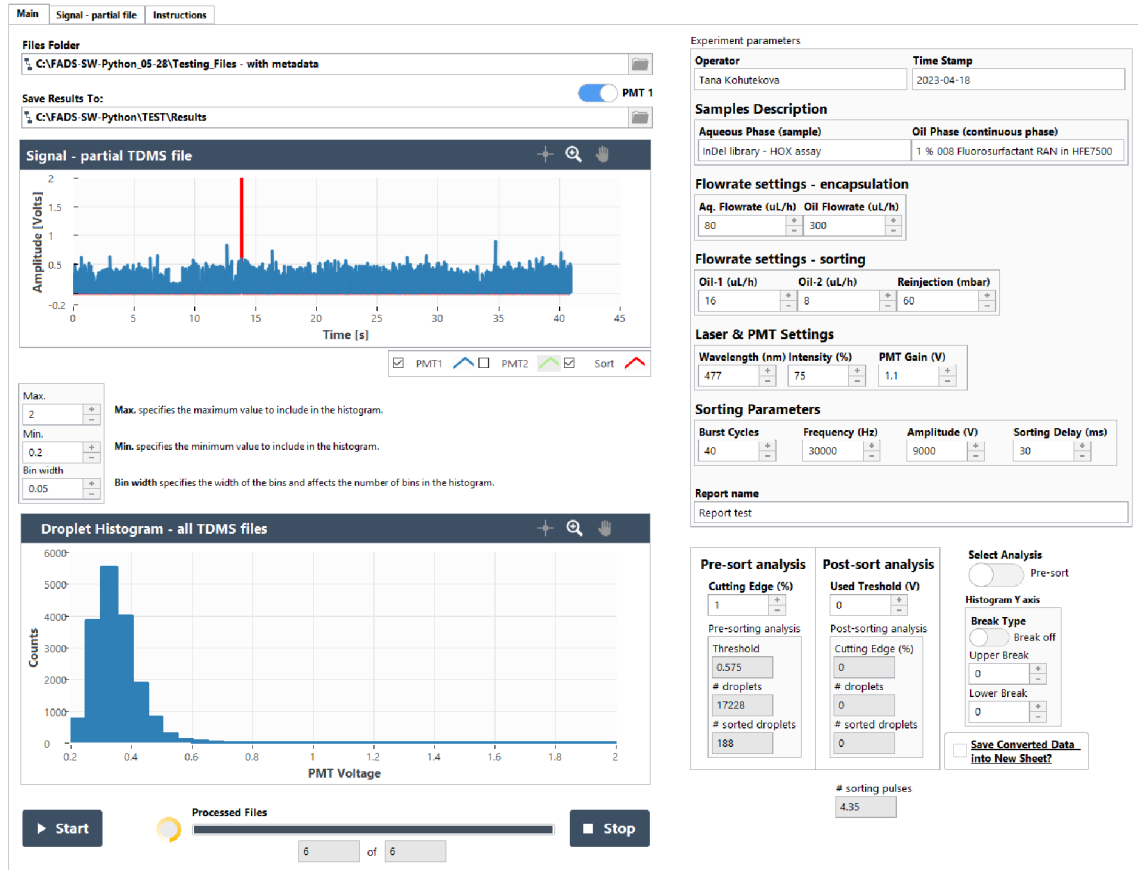


Fig. 5.8: Graphical user interface of Cinderella Analyser for FADS data analysis in LabView.

The user was able to select a folder containing TDMS files and a PMT channel for analysis. The resulting data, including histogram data in *.xls* format, histogram image in *.png* format, and a report in *.pdf* format, are all saved in a separate directory chosen by the user for the results.

Upon loading each TDMS file from the selected directory, the graph was presented to the user. The x-axis showed time, while the y-axis displayed measured voltage from the chosen PMT (blue) and sorting pulses (red).

The user was able to select the parameters of the histogram, which were counted by the Python function, by adjusting the bin width and the range of voltage for analysis. Currently used PMT is able to measure up to 4 V. After each iteration, the histogram for the currently opened TDMS file was displayed, while the x-axis showed voltage and the y-axis displayed count in corresponding

bins. Given that the analysis took some time to complete, and since one experiment was stored in over 100 files, a progress bar was incorporated to display the number of processed files visually and numerically with a moving progress ring.

The GUI of the software was divided into two sections on the right side. When the first TDMS file from the selected folder was loaded into the analyzing software, any metadata contained in the file were also loaded. However, in some cases, previous measurement data either did not have any metadata or the metadata values were left empty.

In order to address this, the software implemented a feature where the loaded metadata parameters with missing values were highlighted and the program was paused, allowing the user to fill in or modify the information for further generation of a report. If the metadata were completely absent from the TDMS file, the corresponding text was highlighted in red. This primarily occurred for the initial measurements or when the acquisition software did not include metadata support. On the other hand, if the metadata fields were present in the TDMS file but were left empty by the user, they were highlighted with a yellow color. This indicated that the metadata existed but still required user input.

If the metadata parameters were filled with information, the software would load and display the corresponding data stored in the TDMS file. These three possibilities (no metadata, empty metadata, filled metadata) are visually illustrated in the Fig.5.9 After completing the edit of the experiment parameters, it was necessary to push Star button to start the analysis or a Stop button to stop the run of the program.

Experiment parameters	
Operator	Time Stamp
	2023.04.18 17:59:27
Samples Description	
Aqueous Phase (sample)	Oil Phase (continuous phase)

Fig. 5.9: Highlighted missing values in GUI of Cinderella Analyser for FADS data analysis in LabView. Red indicated no metadata in the TDMS file, yellow highlight indicated empty metadata and no highlight means that the metadata were present and filled by user.

The lower part was focused on the type of data analysis. With the button, the user could choose whether to analyze the data before actual sorting and thereby calculate the optimal sorting threshold that meets the criteria or to do the final analysis for the whole sorting experiment, respectively.

Since the number of droplets exceeded 10 or even 100 thousand and the goal was mostly to sort the 1 % of the most active, the option with broken axes was added. This button allowed a user to create a histogram with broken axes using a set limit to improve the visualization of the data without losing the information.

In case of any problems with wrong inputs or any other occasions, it was possible to stop the run of the program with the Stop button. After hitting the button, no files were saved.

5.3.3 Steps of analysis

Flowchart of the analyzing software is schematically depicted in Fig. 5.10.

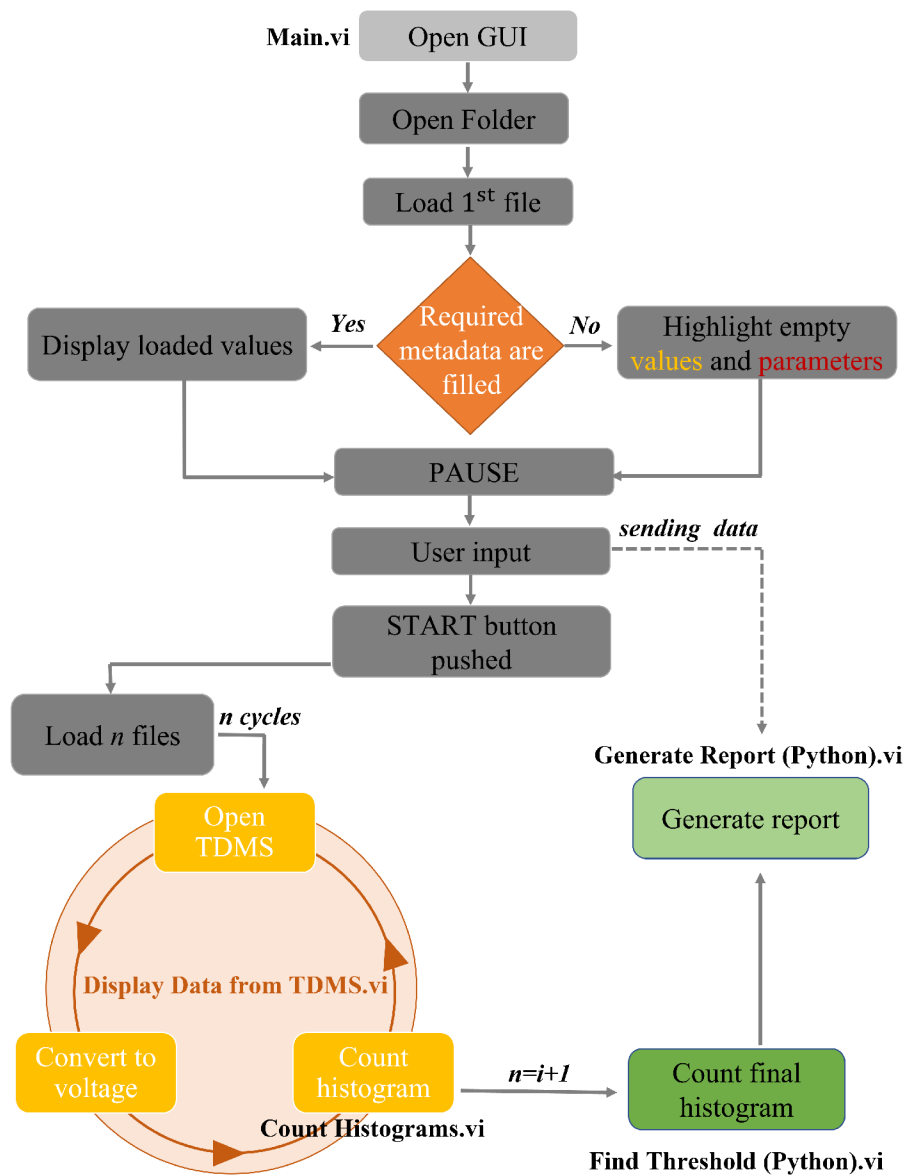


Fig. 5.10: Block scheme of analyzing software.

The analyzing software let the user choose the folder with experimental data and a new folder for saving results. The input parameter for the analysis is the minimal and maximal voltage that the user wanted to analyse and the width of bins in the histogram.

LabView opened the folder and loaded all TDMS files. Then, they were opened and values from the raw signal were recalculated to voltage using a constant for the FPGA card. Data containing PMT1 voltage values were stored in an array, which was an input parameter for the function *CountHistogram* in Python.

This function loaded the array into numpy array and integrated the signal with a window with the length of 150 samples using *FilterPeakDetection* function. The input of the function consisted of a raw signal from one TDMS. The raw signal was smoothed and noise and random high peaks were suppressed while the peaks of interest have been highlighted for easier detection. The position of the peaks was obtained, and the measured values from the raw graph were examined to determine the maximum value within each peak. The indices of the maximum value in the raw signal were returned and used for the calculation of the histogram. The function returned bins and counts in the histogram for all files, while LabView was accumulating the results.

The analysis of sorting experiment data contained two phases: pre-sorting analysis aiming to calculate the threshold for sorting and post-sorting analysis for the analysis of subsequent sorting.

During the first phase, the aim was to determine the optimal sorting threshold based on user preference, meaning to set the desired percentage of sorted droplets from the active ones. Initial measurement was stopped after the detection of 2 000 - 5 000 droplets. The calculations were done by *PreSortingAnalysis* function, where the input consisted of the counted histogram from all TDMS files by the previous step and the cut-off percentage value of active droplets the user aimed to sort. The function returned threshold in volts, number of detected droplets according to detected peaks and number of droplets that would be sorted using calculated threshold. All results were displayed in GUI.

The second phase consisted of sorting using a calculated threshold. At the end of the sorting, the analyzing software enabled to perform post-sorting analysis with similar steps. The difference is, that the inputs for the analysis were histogram and used threshold. The function *PostSortingAnalysis* sums the bins over the set threshold and returns the real percentage of sorted droplets and counts.

Both analyses were done independently and resulted in a PDF report depending on the selected type of analysis. For the analysis of older experiments, the metadata were not included yet, so the user either filled them or in the case of newer files the LabView software loaded them automatically.

Finally, Python script created a PDF report using the function *GenerateReport*. It contained a description of the experiment, final histogram image and calculated results. Histogram data from all files were visualized in Python using the function *ReportGraph*, which created and saved plot with or without broken axes according to the preference of the user with a marked threshold.

The detailed documentation with the block scheme from LabView is in Appendix C and the detection software is available in Appendix D and.

5.4 Analysis of FADS experimental data

5.4.1 Benchmark experiment with fluorescent dye

The first sorting experiment with different concentrations of HPTS showed, that it is possible to distinguish peaks concerning their concentration due to the different fluorescence intensity.

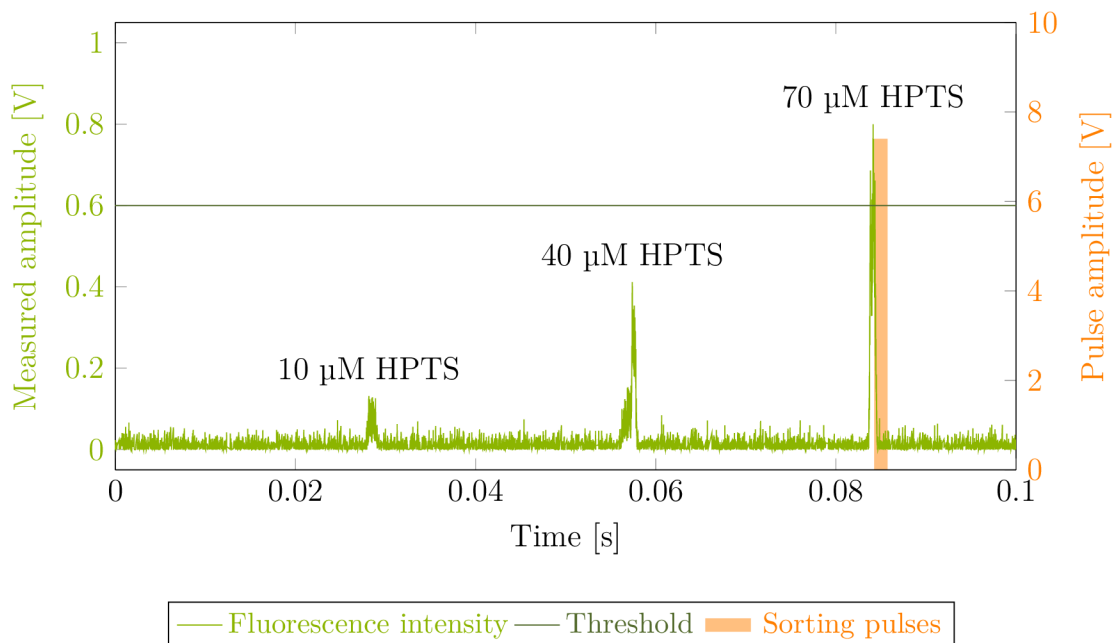


Fig. 5.11: Sample of the signal obtained from benchmark experiment with different concentrations of HPTS. Higher concentration produces a higher amplitude of the signal.

A short segment of the obtained signal is in Fig. 5.11. The main point of the following screening and sorting is to get the variants with the best activity, therefore only droplets with fluorescence above the threshold set to 0.6 V triggered the sorting pulse, which led to a change in the trajectory of a droplet into a collection vial.

5.4.2 Benchmark experiment with mixture of known variants

The benchmark mixture consisted of 50 % of gene-free pIDR9 plasmid, 45 % of ancHLD-RLuc and 5 % of DhaA31, mimicking the InDel library. Droplets with gene free plasmid were not detected with PMT due to the lack of fluorescein. The other two variants were visible to PMT and were detected and sorted.

These data were analyzed with newly created software in LabView and aimed to validate the functionality. The resulting histogram is provided in Fig. 5.12.

The experiment verified the functionality of the FADS system and its sensitivity toward different protein activities. As the DhaA31 ($k_{\text{cat}}=5.85 \text{ s}^{-1}$ [8]) is approximately $20\times$ more active than AncHLD-RLuc ($k_{\text{cat}}=0.29 \text{ s}^{-1}$ [28]) towards DBE substrate, the right population cluster represents mainly the droplets with DhaA31 variants.

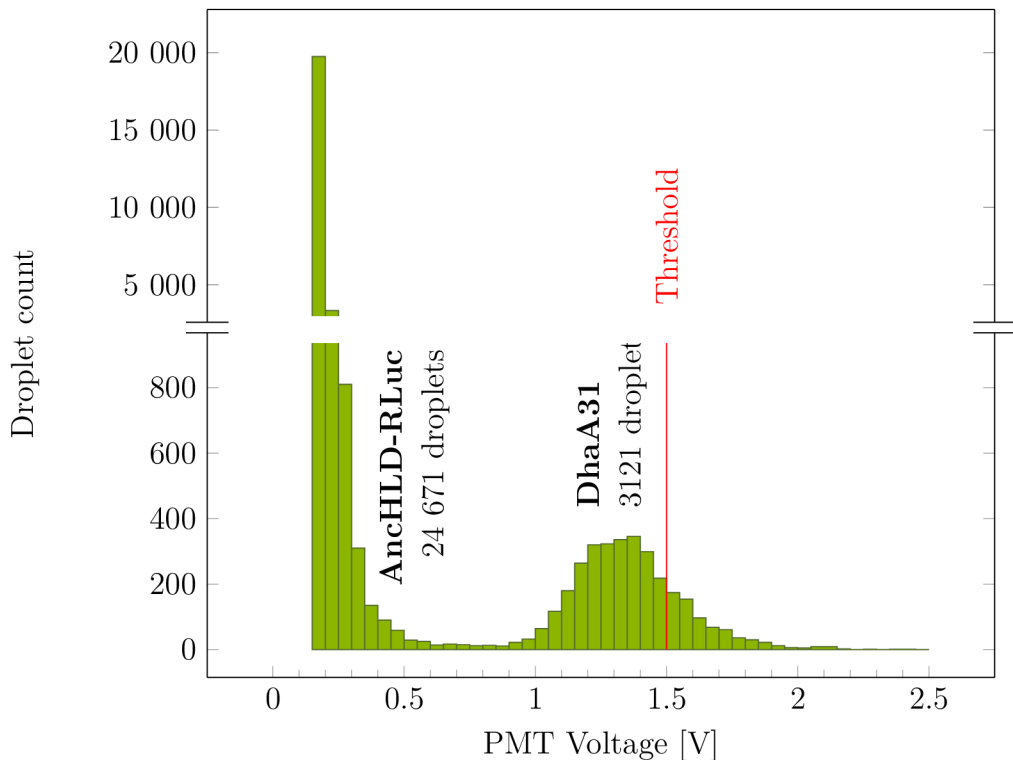


Fig. 5.12: Histogram from benchmark experiment shows 2 populations of active enzymes with different intensities. Red line indicates used sorting threshold.

According to the pre-sorting analysis, the calculated threshold was 1.5 V, which was supposed to enable sorting 1 % of the most active variants. The sorting took around 3 hours due to some impurities in the chip and slower flowrates.

It was expected, that the histogram would contain 2 peaks corresponding to the levels of fluorescence intensities. As the gene free variants are not detected, according

to the theoretical ratio, the ancHLD-RLuc and DhaA31 were supposed to be in a ratio of 1:9. After the analysis of calculated histogram data, it was confirmed that the detected ratio corresponds to the expected outcome. This experiment confirmed that the system is not only able to differentiate the levels of intensity of different variants but is also able to properly detect and analyze data. The parameters of the benchmark experiment mimicked the InDel library.

Sorted droplets were collected into the vial with sterile water for subsequent optimization of amplification by PCR.

5.4.3 InDel library sorting with 1,2-Dibromethane

This experiment was the main goal of this thesis. It aimed to obtain the most active variants from the InDel library.

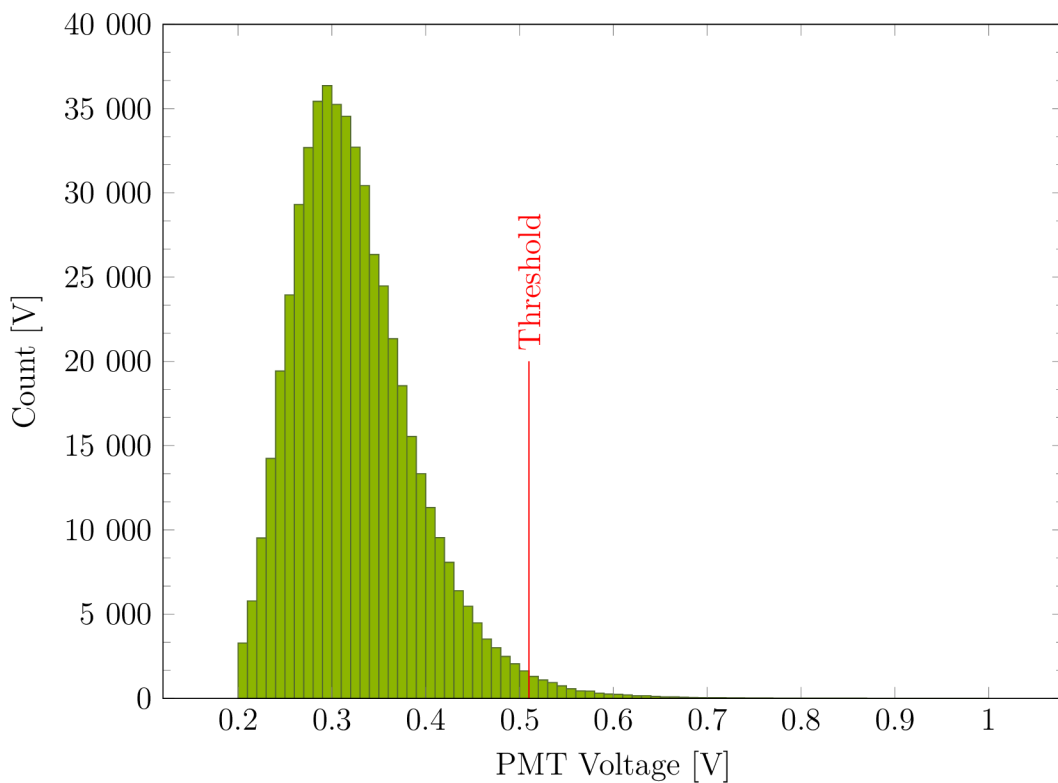


Fig. 5.13: Histogram from measured droplets with InDel library.

The experiment was divided into 2 phases. Initially, after 30 minutes, the pre-sorting analysis was performed, the cut-off value was set to 1 % from active droplets. The calculated threshold was 0.565 V. Full report from the analysis is available in Appendix A.

In the second phase, the calculated threshold was used for sorting the droplets. After 4 hours of sorting, measured data were analyzed.

In the experiment, 528 310 droplets were active and detected. With a used threshold of 0.57 V (adjusted during the experiment), 2 691 droplets were sorted and collected in distilled water for subsequent amplification by PCR and sequencing. The sorted part represented 0.51 % of the total number of detected droplets. The full report from the post-sorting analysis is in Appendix B with the complete setting of the experiment.

Conclusion

The purpose of this bachelor's thesis was to examine the fundamentals of directed evolution and the screening methods associated with large numbers of proteins powered by microfluidics. Microfluidics offers several advantages, including precise control, reduced sample volumes, and high throughput, as microdroplet represents an individual experiment can be generated and analyzed in kHz frequency.

The theoretical aspect of this thesis was foundational to the development of the Fluorescence Activated Droplet Sorting (FADS) system in the Loschmidt Laboratories. The FADS system was equipped with a single photomultiplier for measurement, high-speed and a fluorescent camera for experiment control. These instruments provided the necessary precision and sensitivity for efficient droplet sorting based on fluorescence intensity.

During the initial experiments, chip fabrication and hydrophobic modification were optimized, and suitable conditions were established for subsequent FADS experiments. The newly assembled FADS system underwent many optimization steps to enable a precise and efficient workflow. Laser focusing was performed using fluorescent dye encapsulated in droplets, and benchmark experiments confirmed that it was possible to distinguish different fluorescence intensities.

The large amount of data collected during the sorting process required the creation of software for data analysis. This software allowed users to analyze data before the experiment to calculate the optimal threshold for sorting to meet the requirements. After the experiment, the software allowed users to perform post-sorting analysis and create PDF reports that store the used measurement settings.

With optimized chip fabrication, droplet quality, and sorting system, the InDel library of ancHLD-RLuc protein was sorted to obtain 1 % of the most active variants. Of the total 528 310 droplets, 2 691 fulfilled the sorting criteria and were collected (which represents 0.51 % of active droplets).

The next step in the directed evolution workflow would involve amplification by PCR of sorted variants, followed by subsequent analysis. Additionally, other substrates, such as coumarin or bromhexane, could be used for further sorting.

Overall, the research presented in this thesis provides a comprehensive understanding of directed evolution and its associated screening methods using microfluidics. The findings presented here offer valuable insights into the optimization of the FADS system and data analysis software for future directed evolution experiments.

Bibliography

- [1] Oil In Water And Water In Oil Emulsions: What's The Difference? <https://www.quadroliquids.com/blog/oilinwater-and-waterinoil-emulsions-whats-difference>, 04 2021, accessed: 2023-04-28.
- [2] ALEJALDRE, L.; PELLETIER, J. N.; QUAGLIA, D.: Methods for Enzyme Library Creation: Which one will you choose?: A guide for novices and experts to introduce genetic diversity. *BioEssays*, ročník 43, 08 2021: str. 2100052, doi:10.1002/bies.202100052.
- [3] ASLAN-ÜZEL, A. S.; BEIER, A.; KOVÁŘ, D.; aj.: An Ultrasensitive Fluorescence Assay for the Detection of Halides and Enzymatic Dehalogenation. *ChemCatChem*, ročník 12, 12 2019, doi:10.1002/cctc.201901891.
- [4] BARBER, P. R.; TULLIS, I. D. C.; PIERCE, G. P.; aj.: The Gray Institute 'open' High-content, Fluorescence Lifetime Microscopes. *Journal of Microscopy*, ročník 251, 06 2013: s. 154–167, doi:10.1111/jmi.12057.
- [5] BARET, J.-C.; MILLER, O. J.; TALY, V. A.; aj.: Fluorescence-activated droplet sorting (FADS): Efficient Microfluidic Cell Sorting Based on Enzymatic Activity. *Lab on a Chip*, ročník 9, 07 2009, doi:10.1039/b902504a.
- [6] BHATIA, S.; INGBER, D.: Microfluidic organs-on-chips. *Nature biotechnology*, ročník 32, 08 2014, doi:10.1038/nbt.2989.
- [7] BIDMANOVÁ, S.; CHALOUPKOVÁ, R.; DAMBORSKÝ, J.; aj.: Development of an Enzymatic Fiber-optic Biosensor for Detection of Halogenated Hydrocarbons. *Analytical and Bioanalytical Chemistry*, ročník 398, 11 2010: s. 1891–1898, doi:10.1007/s00216-010-4083-z.
- [8] CHALOUPKOVA, R.; LISKOVA, V.; TOUL, M.; aj.: Light-Emitting Dehalogenases: Reconstruction of Multi-functional Biocatalysts. *ACS Catalysis*, ročník 9, 04 2019, doi:10.1021/acscatal.9b01031.
- [9] COX, J.; FERRIS, L.; THALLADI, V.: Selective Growth of a Stable Drug Polymorph by Suppressing the Nucleation of Corresponding Metastable Polymorphs. *Angewandte Chemie International Edition*, ročník 46, è. 23, 2007: s. 4333–4336, doi:<https://doi.org/10.1002/anie.200605257>, <https://onlinelibrary.wiley.com/doi/pdf/10.1002/anie.200605257>.
URL <https://onlinelibrary.wiley.com/doi/abs/10.1002/anie.200605257>

- [10] DAMBORSKÝ, J.; RORIJE, E.; JESENSKÁ, A.; aj.: Structure–specificity Relationships for Haloalkane Dehalogenases. *Environmental Toxicology and Chemistry / SETAC*, ročník 20, 12 2001: s. 2681–2689, doi:10.1002/etc.5620201205.
- [11] DEMAREE, B.: sorter-code. <https://github.com/AbateLab/sorter-code>. git, 2020.
- [12] HASAN, K.: A mini review of haloalkane dehalogenase: From Molecular Characterization to Applications. *Communications in Science and Technology*, ročník 3, 06 2018: s. 15–18, doi:10.21924/cst.3.1.2018.70.
- [13] IWASAKI, I.; UTSUMI, S.; OZAWA, T.: New Colorimetric Determination of Chloride using Mercuric Thiocyanate and Ferric Ion. *Bulletin of the Chemical Society of Japan - BULL CHEM SOC JPN*, ročník 25, 03 1952: str. 226, doi:10.1246/bcsj.25.226.
- [14] KHALIL, A. S.; COLLINS, J. J.: Synthetic Biology: Applications Come of Age. *Nature Reviews. Genetics*, ročník 11, 05 2010: s. 367–379, doi:10.1038/nrg2775.
- [15] KOUDELÁKOVÁ, T.; BIDMANOVÁ, S.; DVOŘÁK, P.; aj.: Haloalkane Dehalogenases: Biotechnological Applications. *Biotechnology Journal*, ročník 8, 01 2013: s. 32–45, doi:10.1002/biot.201100486.
- [16] KUNKA, A.; DAMBORSKÝ, J.; PROKOP, Z.: *Haloalkane Dehalogenases from Marine Organisms, Methods in Enzymology*, ročník 605. Academic Press, 01 2018, ISBN 9780128150450, s. 203–251, doi:10.1016/bs.mie.2018.03.005.
- [17] LEEMHUIS, H.; KELLY, R. M.; DIJKHUIZEN, L.: Directed evolution of enzymes: Library screening strategies. *IUBMB Life*, ročník 61, è. 3, 2009: s. 222–228, doi:<https://doi.org/10.1002/iub.165>, <https://iubmb.onlinelibrary.wiley.com/doi/pdf/10.1002/iub.165>. URL <https://iubmb.onlinelibrary.wiley.com/doi/abs/10.1002/iub.165>
- [18] LIU, Q.; CHEN, P.; WANG, B.; aj.: Hot Spot Prediction in Protein-protein Interactions by an Ensemble System. *BMC Systems Biology*, ročník 12, 12 2018: s. 12384–12444, doi:10.1186/s12918-018-0665-8.
- [19] LOS, G. V.; ENCELL, L. P.; MCDUGALL, M. G.; aj.: HaloTag: A Novel Protein Labeling Technology for Cell Imaging and Protein Analysis. *ACS chemical biology*, ročník 3, 07 2008: s. 373–382, doi:10.1021/cb800025k.

- [20] MAZUTIS, L.; GILBERT, J.; UNG, W.; aj.: Single-cell Analysis and Sorting Using Droplet-based Microfluidics. *Nature Protocols*, ročník 8, 04 2013: s. 870–891, doi:10.1038/nprot.2013.046.
- [21] SAVINO, S.; DESMET, T.; FRANCEUS, J.: Insertions and Deletions in Protein Evolution and Engineering. *Biotechnology Advances*, ročník 60, 06 2022, doi:10.1016/j.biotechadv.2022.108010.
- [22] SCHENKMAYEROVÁ, A.; PINTO, G. P.; TOUL, M.; aj.: Engineering the Protein Dynamics of an Ancestral Luciferase. *Nature Communications*, ročník 12, 06 2021, doi:10.1038/s41467-021-23450-z.
- [23] SCHÜTZ, S. S.; BENEYTON, T.; BARET, J.-C.; aj.: Rational Design of a High-throughput Droplet Sorter. *Lab on a Chip*, ročník 19, 06 2019, doi:10.1039/C9LC00149B.
- [24] SCOTT, S.; ALI, Z.: Fabrication Methods for Microfluidic Devices: An Overview. *Micromachines*, ročník 12, 03 2021: str. 319, doi:10.3390/mi12030319.
- [25] TARN, M. D.; PAMME, N.: *Reference Module in Chemistry, Molecular Sciences and Chemical Engineering*. Elsevier, 2014, ISBN 978-0-12-409547-2, doi:10.1016/B978-0-12-409547-2.05351-8.
- [26] TERRY, S. C.; JERMAN, H. J.; ANGELL, J. B.: A Gas Chromatograph Air Analyzer Fabricated on a Silicon Wafer. *Electron Devices on IEEE Transactions*, ročník 26, 01 1980: s. 1880–1886, doi:10.1109/T-ED.1979.19791.
- [27] VALLEJO, D.; NIKOOMANZAR, A.; PAEGEL, B. M.; aj.: Fluorescence-Activated Droplet Sorting for Single-Cell Directed Evolution. *ACS Synthetic Biology*, ročník 8, 05 2019: s. 1430–1440, doi:10.1021/acssynbio.9b00103.
- [28] VASINA, M.: Panoramic view on steady-state kinetics of wild type and engineered HLDs. *Internal Progress Report: unpublished*, 2022.
- [29] WANG, Y.; XUE, P.; CAO, M.; aj.: Directed Evolution: Methodologies and Applications. *Chemical Reviews*, ročník 121, 07 2021, doi:10.1021/acs.chemrev.1c00260.
- [30] WESTERBEEK, A.; SZYMAŃSKY, W.; WIJMA, H. J.; aj.: Kinetic Resolution of α -Bromoamides: Experimental and Theoretical Investigation of Highly Enantioselective Reactions Catalyzed by Haloalkane Dehalogenases. *Advanced Synthesis & Catalysis*, ročník 353, 04 2011: s. 931–944, doi:10.1002/adsc.201000726.

- [31] YE, L.; YANG, C.; YU, H.: From Molecular Engineering to Process Engineering: Development of High-throughput Screening Methods in Enzyme Directed Evolution. *Applied Microbiology and Biotechnology*, ročník 102, 01 2018: s. 559–567, doi:10.1007/s00253-017-8568-y.
- [32] ZAMORA, R.; MARTINEZ-PASTOR, J.; FAURA, F.: Thermal, Viscoelastic and Surface Properties of Oxidized Field's Metal for Additive Microfabrication. *Materials*, ročník 14, 12 2021, doi:10.3390/ma14237392.

Symbols and abbreviations

APF	Aminophenyl fluorescein
DNA	Deoxyribonucleic acid
<i>E. coli</i>	<i>Escherichia coli</i>
ETH	Eidgenössische Technische Hochschule Zürich
FACS	Fluorescence-Activated Cell Sorting
FADS	Fluorescence-Activated Droplet Sorting
FITC	Fluorescein Isothiocyanate
FPGA	Field Programmable Gate Arrays
FOTS	(1 <i>H</i> ,1 <i>H</i> ,2 <i>H</i> ,2 <i>H</i> -perfluorooctyl)silane
GC	Gas Chromatography
GUI	Graphical User Interface
HLD	Haloalkane Dehalogenases
HOX	Halide Oxidation Assay
HPTS	8-hydroxy-1,3,6-pyrenetrisulfonic acid trisodium salt
InDel	Insertion and Deletion
LB	Luria-Bertani liquid medium
LL	Loschmidt Laboratories
LOC	Lab-on-chip
MS	Mass Spectrometry
OD	Optical Density
O/W	Oil-in-water
PCR	Polymerase Chain Reaction
PDMS	Poly-Dimethyl Siloxane
pH	potential of Hydrogen

PMT	Photomultiplier Tube
RID	Random Insertion and Deletion Mutagenesis
SOC	variant of Super Optimal broth with Catabolite repression
ssDNA	Single Strand DNA
TCPS	Trichloro(1 <i>H</i> ,1 <i>H</i> ,2 <i>H</i> ,2 <i>H</i> -perfluorooctyl)silane
W/O	Water-in-oil

List of appendices

A	Pre-sorting report from InDel sorting	65
B	Post-sorting report from InDel sorting	67
C	LabView-Python software documentation	69
D	Electronic supplement	88
	D.1 LV-Project	88
	D.2 Reports	88

A Pre-sorting report from InDel sorting

Sorting Protocol Calculation of estimated threshold

Name: Tana Kohutekova

Date: 2023-04-18

Samples description

Oil Phase 1 % 008 Fluorosurfactant RAN in HFE7500

Aqueous Phase InDel library - HOX assay

Flowrate Settings

Encapsulation Oil Flowrate 80 uL/hour

Aqueous Flowrate 300 uL/hour

Sorting Flowrates Oil Phase 1 16 uL/hour

Oil Phase 2 8 uL/hour

Reinjection 60 mBar

Sorting Parameters

Laser Wavelength 477 nm

Laser Intensity 75 %

PMT Gain 1.1 V

Burst Cycles 40

Pulse Amplitude 9000 V

Frequency 30000 Hz

Sorting Delay 30 us

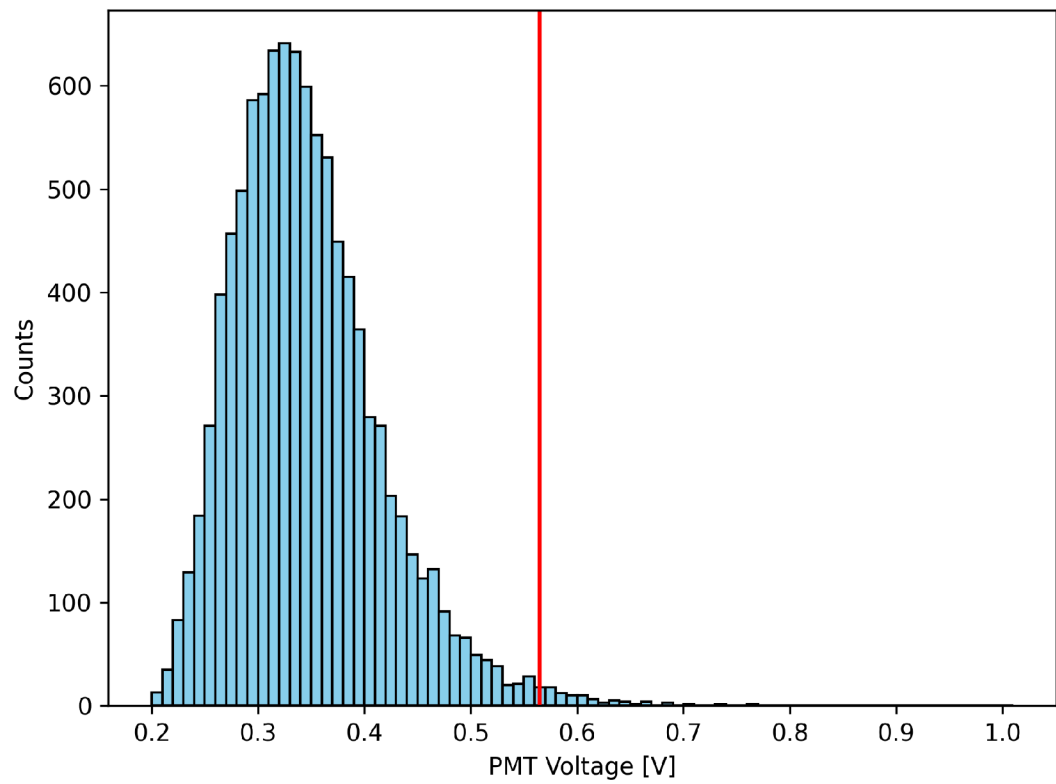
Cutting Edge 1 %

Estimated Threshold 0.565 V

Sorting Protocol

Calculation of estimated threshold

Results



Total number of droplets 9926

B Post-sorting report from InDel sorting

Sorting Protocol Calculation of sorted droplets



Name: Tana Kohutekova

Date: 2023-04-18

Samples description

Oil Phase 1 % 008 Fluorosurfactant RAN in HFE7500

Aqueous Phase InDel library - HOX assay

Flowrate Settings

Encapsulation Oil Flowrate 80 uL/hour

Aqueous Flowrate 300 uL/hour

Sorting Flowrates Oil Phase 1 16 uL/hour

Oil Phase 2 8 uL/hour

Reinjection 60 mBar

Sorting Parameters

Laser Wavelength 477 nm

Laser Intensity 75 %

PMT Gain 1.1 V

Burst Cycles 40

Pulse Amplitude 9000 V

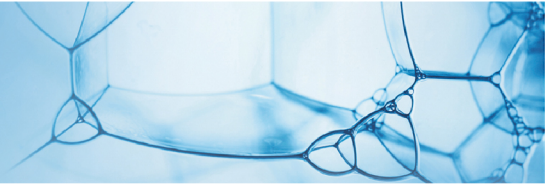
Frequency 30000 Hz

Sorting Delay 30 us

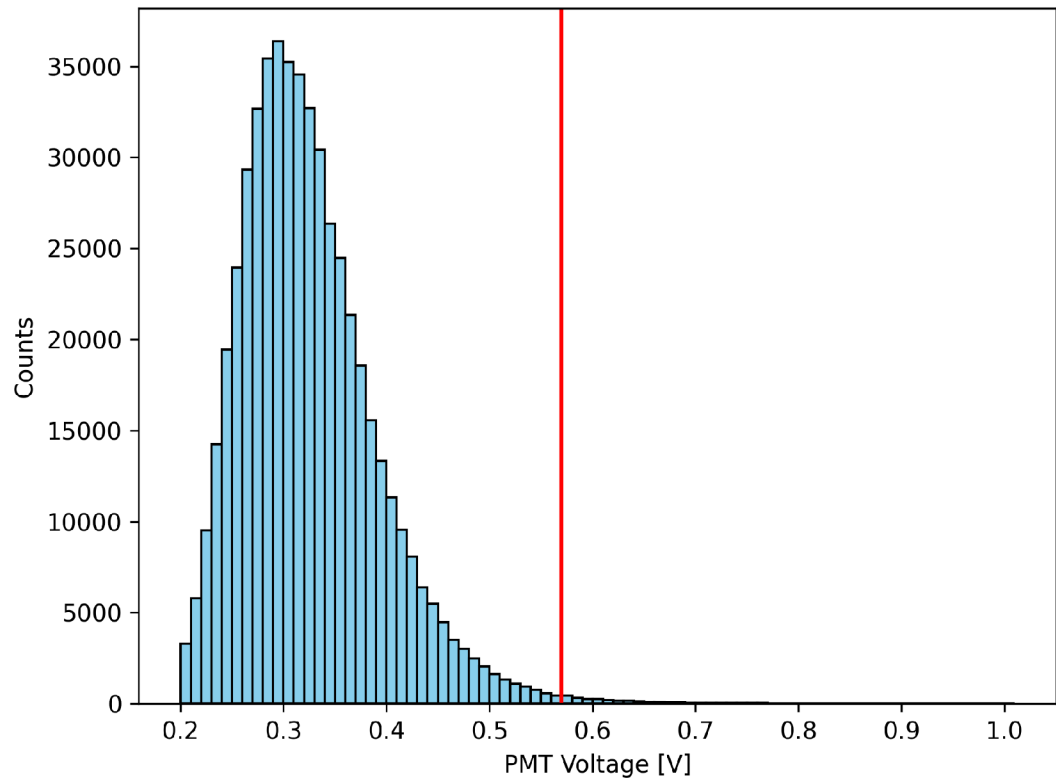
Used Threshold 0.57 V

Sorting Protocol

Calculation of sorted droplets



Results



Total number of droplets	528310
Sorted droplets	2691
Percentage	0.51 %

C LabView-Python software documentation

This documentation is also a manual to Cinderella Analyser - software for FADS data analysis. It provides data visualization, pre-sorting and post-sorting analysis and generates report in PDF.

Program is created in LabView2019 bundled with Python functions. LabView2019 supports only version 3.6 of Python, therefore this version was used as an interpreter.

Cinderella Analyser



The Fluorescence-Activated Droplet Sorting (FADS) technique produces extensive data sets requiring automatic and high throughput analysis. The application sequentially opens all the .tdms files in the specified folder, converts raw signals saved in the .tdms files to voltage values, detects droplet peaks, and does mathematical analysis with final histogram plotting. It combines LabVIEW and Python into a highly efficient and scalable SW tool.

Workflow

Open the Folder with all the .tdms files you want to analyze (click on the **Files Folder**, select a specific folder with your data, and click the **Current Folder** button).

The resulting data, including histogram data in .xlsx format, histogram image in .png format, and a report in .pdf format, are all saved in a separate directory chosen by the user for the results via **Save Results To:**

Based on the Sorting experiment, you can estimate the range values (**Max.** and **Min.**) for the histogram and adjust the **Bin width** and **Select Analysis**.

Once the **Save Converted Data into New Sheet?** is checked, a new sheet (TDMS group) with converted data will be created into each .tdms file; hence all metadata will be available in the original place.

Run the software. It automatically detects missing experimental parameters (metadata) and highlights them. Fulfill the missing **Experiment Parameters**, **Start** the analysis, and wait until all files are analyzed, and the .pdf report is generated.

The program stops whenever all files in the folder are processed, or the user clicks **STOP** (this might take a while).

In case of trouble, check the **Error OUT** cluster and contact the authors.

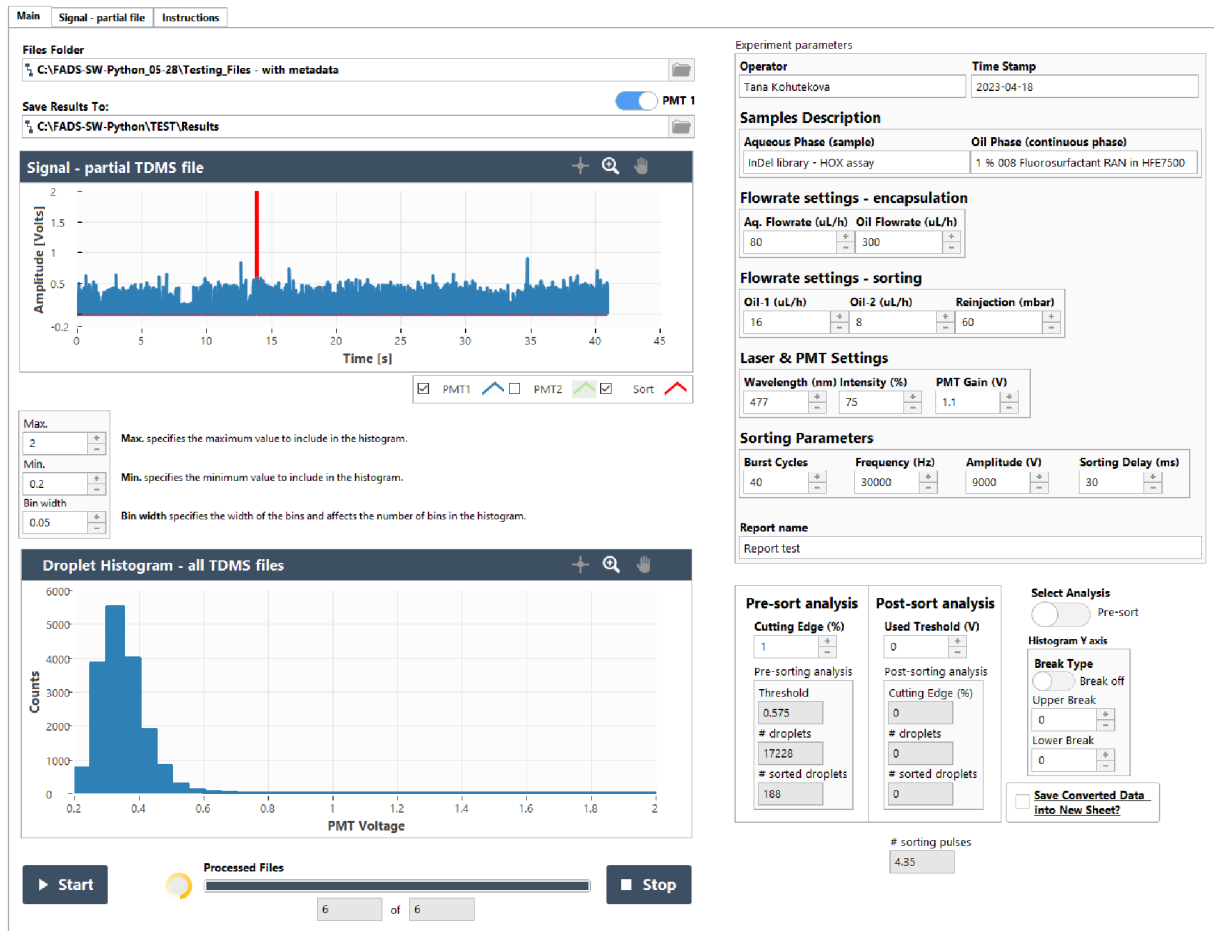


Figure 1: GUI of the Cinderella Analyser under running analysis.

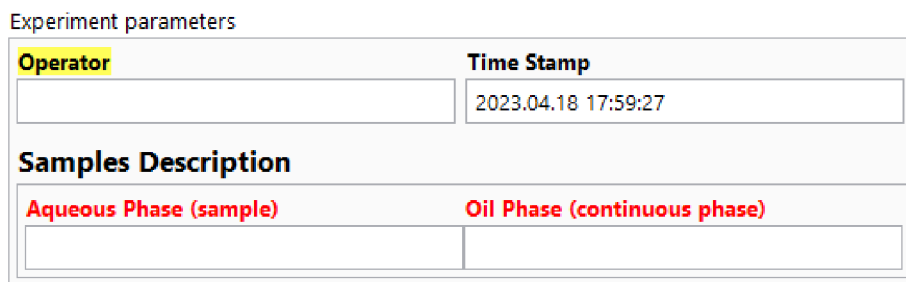


Figure 2: Highlighted missing parameters.
Red: no metadata, Yellow: empty metadata, Without highlight: filled metadata

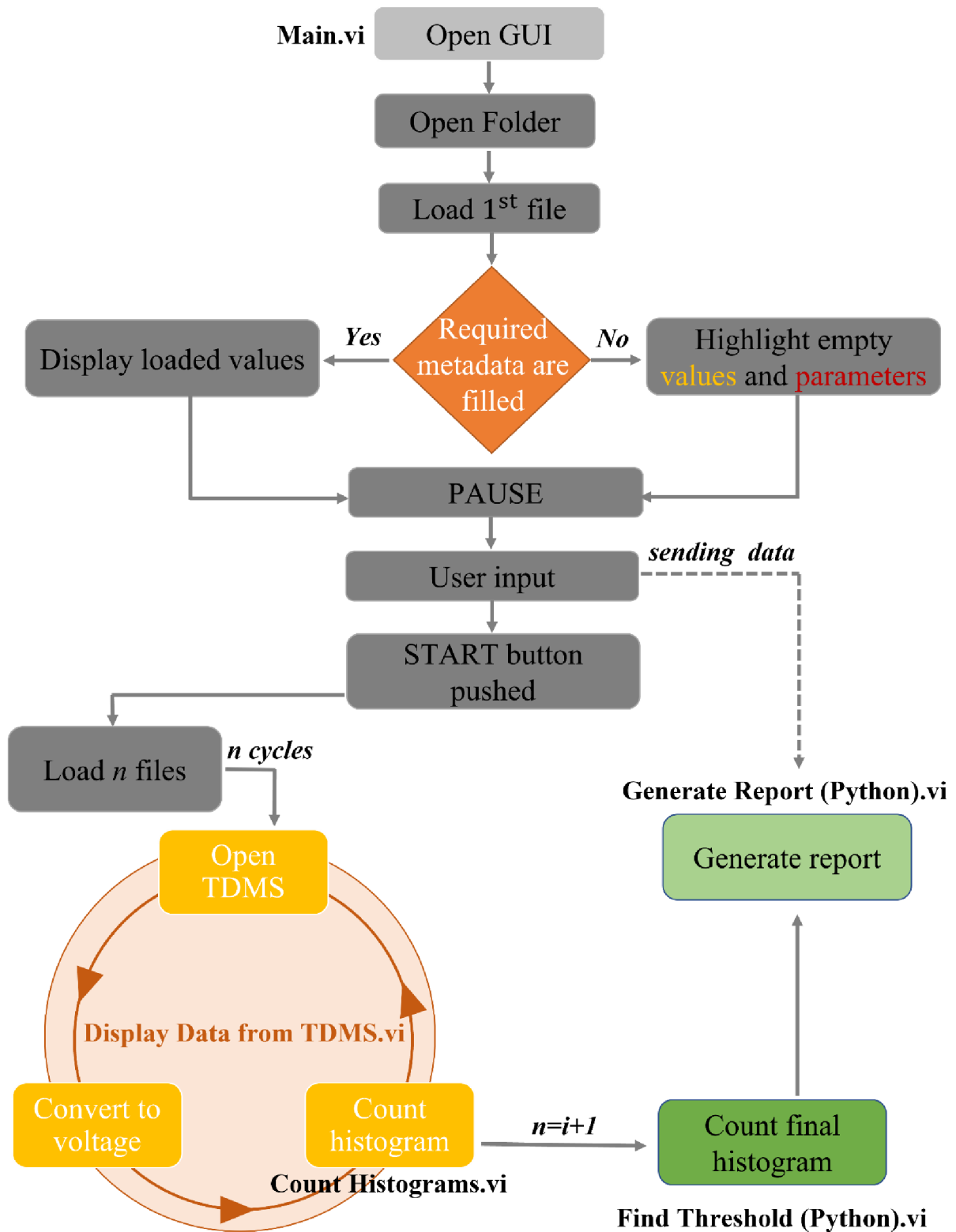


Figure 3: Scheme of the actions provided by the software.

Loading the files for the analysis

Files Folder

Z:_DataStorage\FADS-Sorter\2023-04-18_InDel_8000DBE\Sorting

Save Results To: PMT 1

Z:_DataStorage\FADS-Sorter\2023-04-18_InDel_8000DBE\Sorting_Results

Files Folder

Select a folder with .tdms data files for the analysis.

PMT selector

Select which one of the PMT signal channels will be analyzed. It does not affect the visualization of the data in the **Signal** chart.

Save Results To:

Specify the folder where the results and protocol will be saved.

Histogram settings

Max. 1	Max. specifies the maximum value to include in the histogram.
Min. 0.2	Min. specifies the minimum value to include in the histogram.
Bin width 0.01	Bin width specifies the width of the bins and affects the number of bins in the histogram.

Max.

Specifies the maximum value to include in the histogram.

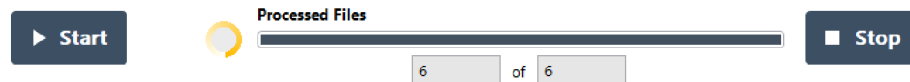
Min.

Specifies the minimum value to include in the histogram.

Bin width

Specifies the width of the bins and affects the number of bins in the histogram.

Progress of the analysis and STOP button



Progress Ring

If the ring is moving, the program is processing data.

Processed Files

The progress bar relates to the processed number of files shown below in the numerical indicators that display the number of processed files from the overall number of files included in the analysis.

Stop Button

The program stops under the standard way when all the files in the queue are analyzed. The running analysis may also be interrupted by pressing the STOP button. This is helpful when any settings must be changed, and the files must be reanalyzed with the new parameters. In that case, data and pdf report will not be saved. Stopping the analysis may take a while if the math process is running.

Start Button

After filling or changing the metadata, it is necessary to start the analysis. Analysis may take a while.

Experiment Parameters

Operator	Time Stamp
Tana Kohutekova	2023-04-18
Samples Description	
Aqueous Phase (sample)	Oil Phase (continuous phase)
InDel library - HOX assay	1 % 008 Fluorosurfactant RAN in HFE7500

Operator

Name of the experimentalist.

Time Stamp

Date of the beginning of the experiment. If there is an overnight experiment, use the first date.

Sample Description – Aqueous Phase (sample)

Description of the aqueous dispersed phase.

Sample Description – Oil Phase (continuous phase)

Description of the continuous oil phase.

Flowrate settings – encapsulation

Flowrate settings - encapsulation

Aq. Flowrate (uL/h)	Oil Flowrate (uL/h)
300	80

Aq. Flowrate (mL/h)

Flowrate of the dispersed aqueous phase on the encapsulation chip.

Oil Flowrate (mL/h)

Flowrate of the continuous oil phase on the encapsulation chip.

Flowrate settings – sorting

Flowrate settings - sorting

Oil-1 (uL/h)	Oil-2 (uL/h)	Reinjection (mbar)
16	8	60

Oil-1 (mL/h)

Flowrate of the oil applied on the inlet further from the electrodes.

Oil-2 (mL/h)

Flowrate of the oil applied on the inlet closer to the electrodes.

Reinjection (mbar)

Pressure applied on the droplets coming from the reservoir to the sorting chip.

Laser & PMT Settings

Laser & PMT Settings		
Wavelength (nm)	Intensity (%)	PMT Gain (V)
477	75	1.1

Wavelength (nm)

Specify the wavelength of the used laser.

Intensity (%)

Specify the intensity of the laser used.

PMT Gain (V)

Specify the used Control Voltage for the Gain on the PMT. The range can vary between 0.5 to 1.1 V.

Sorting Parameters

Sorting Parameters			
Burst Cycles	Frequency (Hz)	Amplitude (V)	Sorting Delay (μ s)
40	30000	9000	30

Burst Cycles

A number of generated dielectrophoretic pulses.

Frequency (Hz)

Frequency of generated dielectrophoretic pulses.

Amplitude (V)

The amplitude of generated dielectrophoretic pulses.

Sorting Delay (ms)

Sorting Delay between the droplet detection and generation of dielectrophoretic pulses.

Report Name

Report name
2023-04-18 Post-Sorting Analysis

Specify the name of the report. Playing it safe and avoiding common illegal filenames and directory characters is essential.

Pre-sort and Post-sort Analysis – inputs

Cutting Edge (%)

Define the cutting edge as a percentage of the droplets you want to sort. Typically, between 0.5-5 %.

Used Threshold (V)

Define the threshold voltage used for the sorting.

Pre-sort analysis	Post-sort analysis
Cutting Edge (%) <input type="text" value="1"/>	Used Threshold (V) <input type="text" value="0.57"/>
Pre-sorting analysis Threshold <input type="text" value="0"/>	Post-sorting analysis Cutting Edge (%) <input type="text" value="0"/>
# droplets <input type="text" value="0"/>	# droplets <input type="text" value="0"/>
# sorted droplets <input type="text" value="0"/>	# sorted droplets <input type="text" value="0"/>

Pre-sort Analysis – outputs

Threshold

Calculated threshold as average from 2 bins close to the cutting-edge value. Value “-999” indicates an error during the process. Check the Settings and restart the Program.

droplets

Calculated the number of droplets (peaks) detected by the SW. Value “-999” indicates an error during the process. Check the Settings and restart the Program.

sorted droplets

A number of sorted droplets based on the total counts from the bins close to the cutting-edge value. Value “-999” indicates an error during the process. Check the Settings and restart the Program.

Pre-sort Analysis – outputs

Cutting Edge (%)

It is calculated cutting edge percentage from the sorted droplets. Value “-999” indicates an error during the process. Check the Settings and restart the Program.

droplets

Calculated the number of droplets (peaks) detected by the SW. Value “-999” indicates an error during the process. Check the Settings and restart the Program.

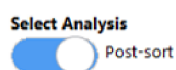
sorted droplets

A number of sorted droplets based on the total counts from the bins close to the cutting-edge value. Value “-999” indicates an error during the process. Check the Settings and restart the Program.

sorting pulses

A number of sorted droplets based on the number of generated dielectrophoretic pulses. Value “-999” indicates an error during the process. Check the Settings and restart the Program.

Select Analysis



Select the detection method and the template for the final protocol.

Histogram Y axis

Histogram Y axis

Break Type

Break on Break off

Upper Break

0

Lower Break

0

Break Type

Select “Break on” if you want to split the asymmetric histogram; otherwise, select “Break off”.

Upper Break

Define the Upper break limit if you want to split the asymmetric histogram.

Lower Break

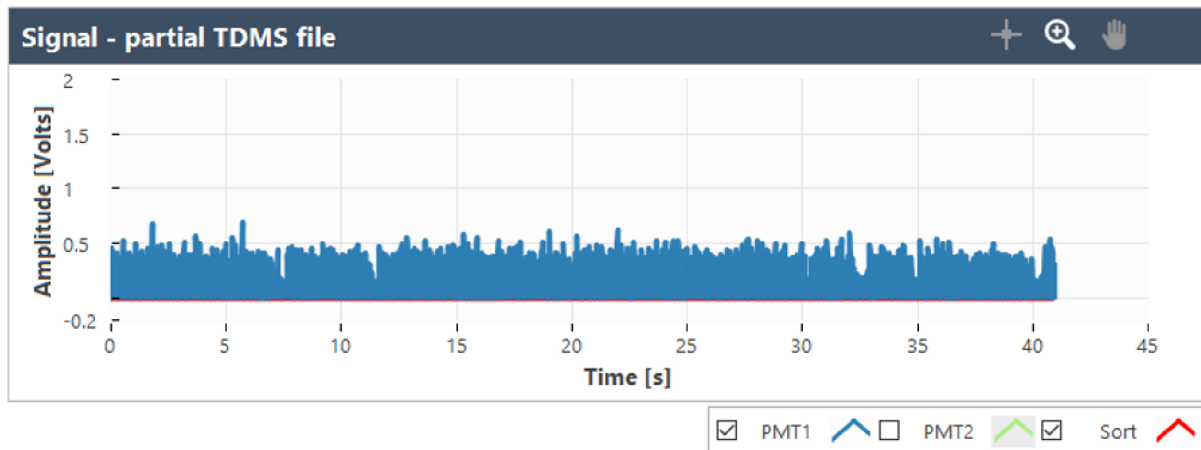
Define the Lower break limit if you want to split the asymmetric histogram.

Save Voltages

Save Converted Data into New Sheet?

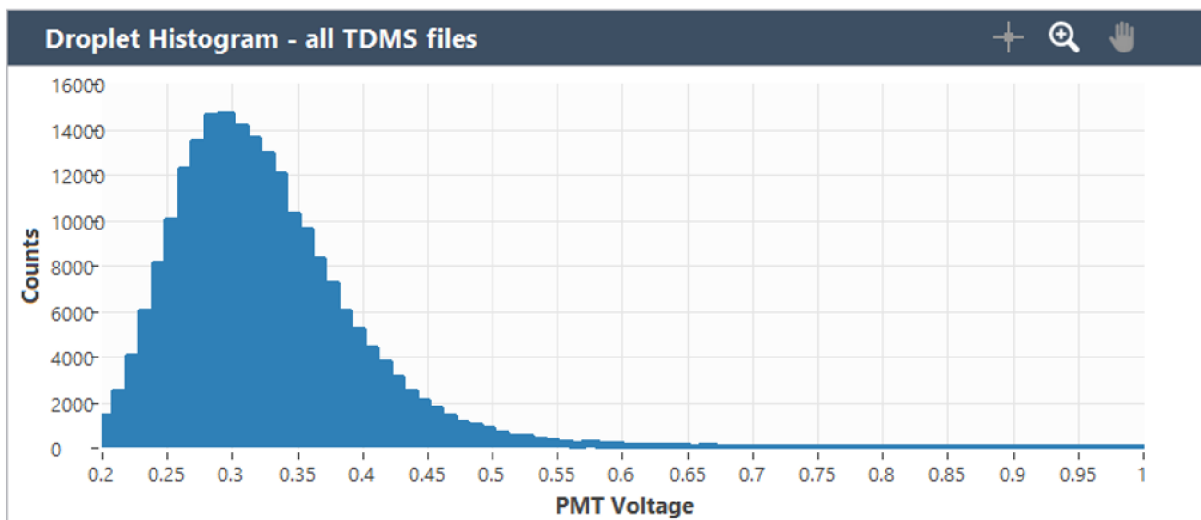
Once the **Save Converted Data into New Sheet?** is checked, a new sheet (TDMS group) with converted data will be created into each particular .tdms file, and hence all metadata will be available in the original place.

Signal - partial TDMS file



Plots the signals and sorting channels of processed .tdms file. In the **Plot Legend**, use the checkbox to select which plots you want to display in the plot area. The “Signal – partial file” tab shows a broader graph view in the “**Main**” tab. The graphs are also exported as .bmp files into the folder containing the original .tdms files.

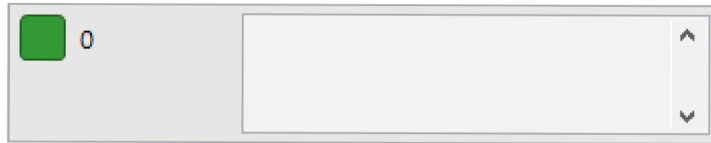
Droplet Histogram - all TDMS files



Displays a growing histogram based on the already analyzed .tdms. files.

Error OUT

Error OUT



In the case of any error, the **Status** is red, and a numerical value indicates the **Error Code**. **Error Description[source]** describes the origin of the error or warning.

Right-click the **error in** control on the front panel and select **Explain Error** or **Explain Warning** from the shortcut menu for more information about the error.

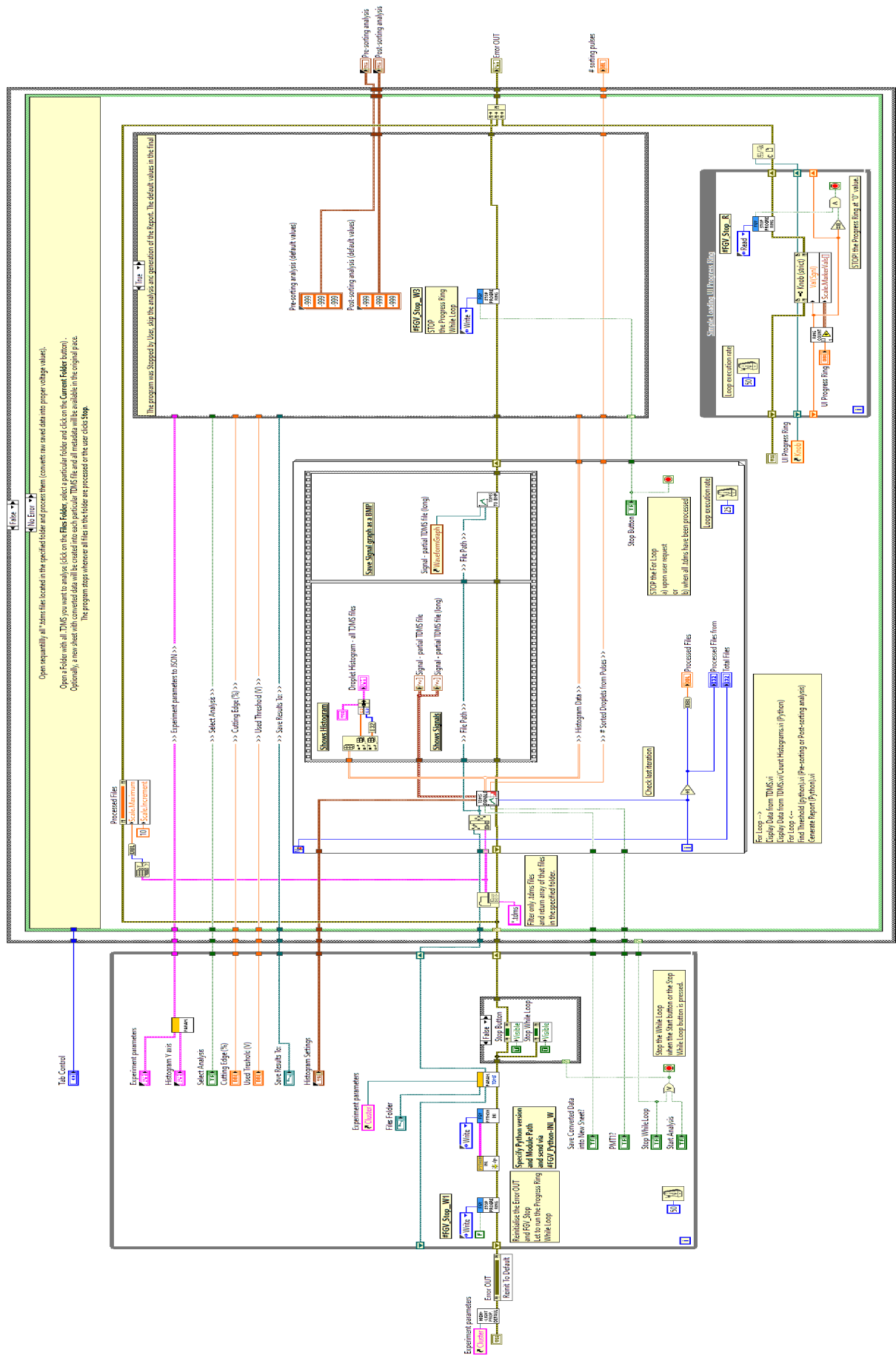


Figure 4: Block diagram of the Main.vi

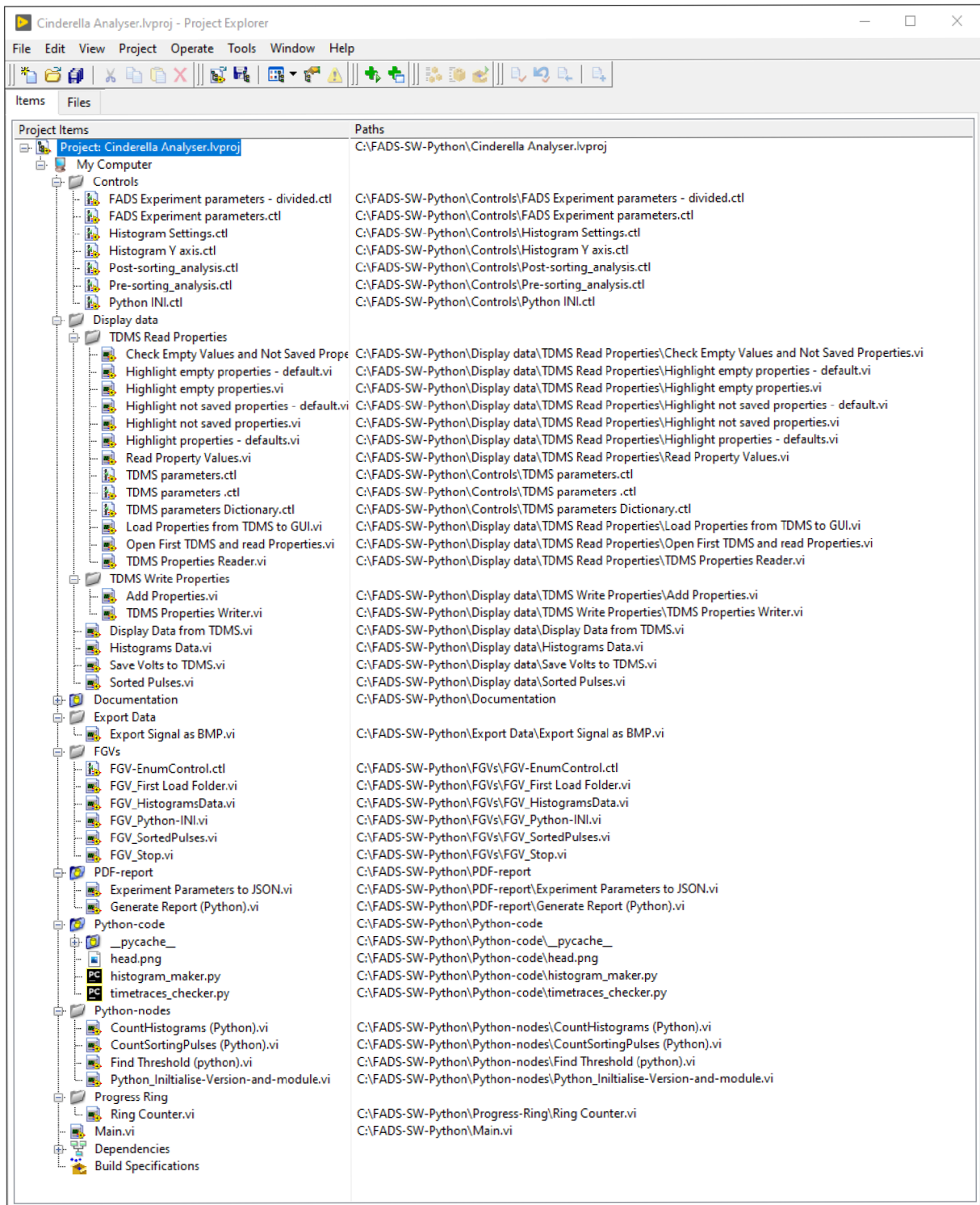



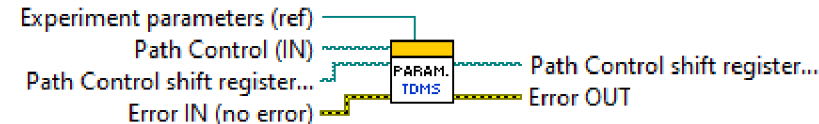
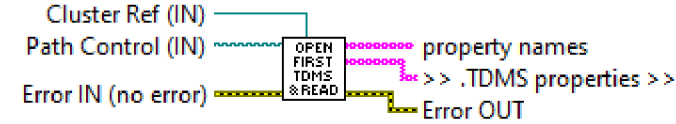
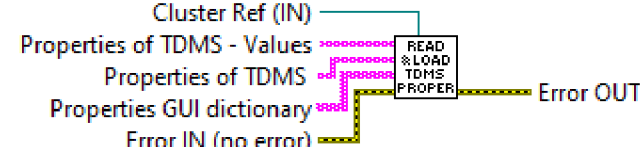
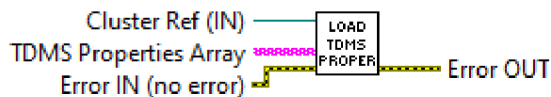


Figure 5: LabVIEW Project Explorer with the Cinderella Analyser project items.

The list of subVIs

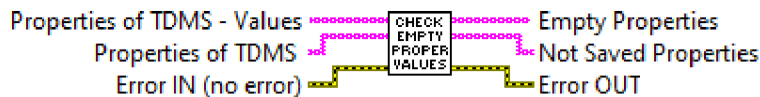
	<p>Python_Initialise-Version-and-module.vi</p>  <p>Specify the installed version of Python and the Module path. These general inputs will be send via FGV to all Python nodes used throughout the application..</p> <p>C:\FADS-SW-Python\Python-nodes\Python_Initialise-Version-and-module.vi</p>
	<p>TDMS Properties Reader.vi</p>  <p>Load first .TDMS file from the selected folder. Find an appropriate controls with empty Parameters in the TDMS file and highlight them in the Experiment parameters in the main GUI.</p> <p>C:\FADS-SW-Python\Display data\TDMS Read Properties\TDMS Properties Reader.vi</p> <p>Open First TDMS and read Properties.vi</p>  <p>Filter only .TDMS files and return array of that files of the specified folder. Load first .TDMS file from the selected folder and read its properties.</p> <p>Read Property Values.vi</p>  <p>Look for Properties saved in the TDMS and identify those with empty values and get the array of those Properties with empty values. Compare the list of all wanted Properties and identify those not saved in the TDMS file, and get the array of those Not Saved Properties</p>

Load Properties from TDMS to GUI.vi



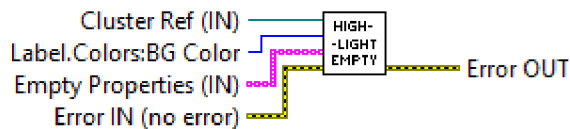
If data exists, load the Properties of TDMS into Experiment Parameters in the main GUI.
Iterate for all Controls included in the Experiment parameters cluster of GUI .

Check Empty Values and Not Saved Properties.vi



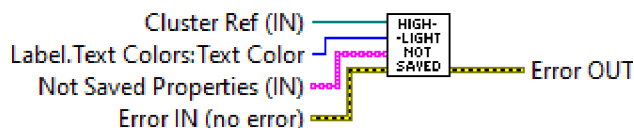
Look for Properties saved in the TDMS and identify those with empty values and get the array of those Properties with empty values.
Compare the list of all wanted Properties and identify those not saved in the TDMS file, and get the array of those Not Saved Properties

Highlight empty properties.vi



In the Experiment parameters, find an appropriate controls with empty Parameters in the TDMS file and highlight them.s

Highlight not saved properties.vi



In the Experiment parameters, highlight not originally saved TDMS properties.

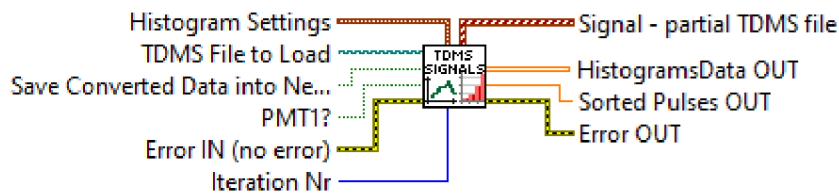
Highlight properties - defaults.vi



Reinitialise colours of all labels and backgrounds in the Experiment Parameters cluster.



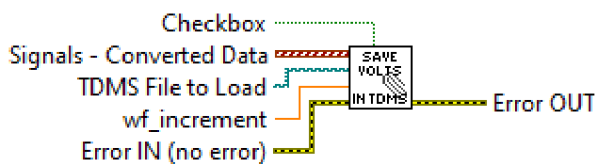
Display Data from TDMS.vi



Opens .tdms file and reads time traces from specified channels - PMT1, PMT2, and Sorting Pulses. Converts the data into voltages (optionally saves them) and calculates partial histogram data as well as the sorted droplets based on the pulses.

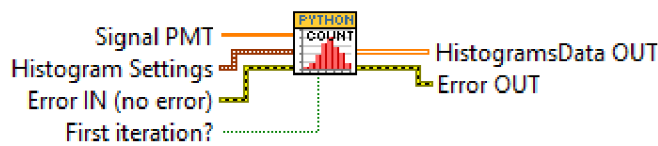
C:\FADS-SW-Python\Display data\Display Data from TDMS.vi

Save Volts to TDMS.vi



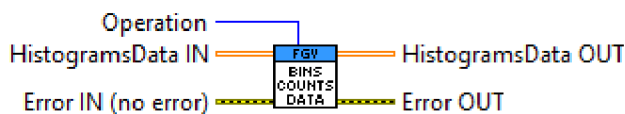
Based on the user choice, saves converted data (voltages) into a new group of the same appropriate .tdms file.

CountHistograms (Python).vi



Proceed with the Python code for the calculation of partial Histogram data and send the calculated values to the GUI and store them in the FGV.

FGV_HistogramsData.vi



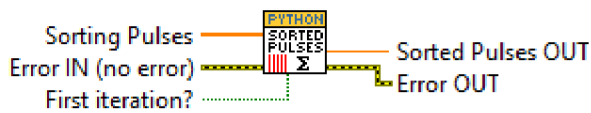
This FGV stores the Histogram Data.

Histograms Data.vi



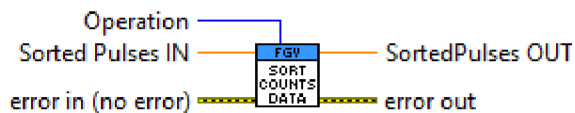
Sums up the partial Histogram Data and stores the data in the FGV.

CountSortingPulses (Python).vi



Proceed with the Python code for the calculation of sorted droplets and send the calculated values to the GUI and store them in the FGV.

FGV_SortedPulses.vi



This FGV stores the value of Sorted Pulse calculated from the series of dielectrophoretic pulses..

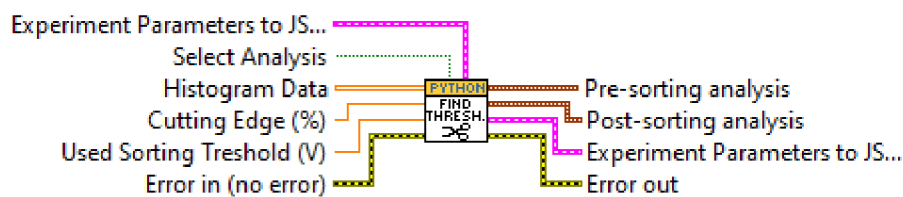
Sorted Pulses.vi



Computes the sum of the value taken from previous iteration of FGV and the latest value from Python node.



Find Threshold (python).vi

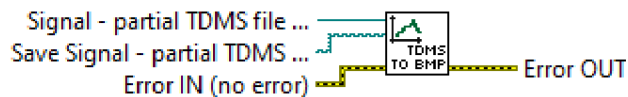


Proceed with the Python code either for the Presorting or PostSorting Analysis and send the calculated values to the GUI and to the JSON text as input for the generation of a Report.

C:\FADS-SW-Python\Python-nodes\Find Threshold (python).vi








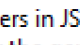




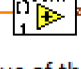








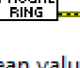



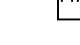
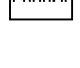





Export Signal as BMP.vi



Load the name of a *.TDMS file and do export of the graph as a *.BMP file.

C:\FADS-SW-Python\Export Data\Export Signal as BMP.vi

	<p align="center">Generate Report (Python).vi</p> <p>Save Histogram Data To:  Error OUT</p> <p> Histogram Data   Error OUT</p> <p> Sorting Parameters   Error OUT</p> <p> Error IN (no error)   Error OUT</p> <p>Converts all the paramaters in JSON string and proceed with the Python code for the generation of the PDF report from the FADS sorting.</p> <p>C:\FADS-SW-Python\PDF-report\Generate Report (Python).vi</p>
	<p align="center">Ring Counter.vi</p> <p>t in   t out</p> <p>UI Progress Ring   Scale.Marker Values[]</p> <p>Counter raises the value of the Progress Ring and culminates the value in the range between 0 and 100 %.</p> <p>C:\FADS-SW-Python\Progress-Ring\Ring Counter.vi</p>
	<p>FGV-EnumControl.ctl</p> <p>C:\FADS-SW-Python\FGVs\FGV-EnumControl.ctl</p>
	<p>FGV_Python-INI.vi</p> <p>C:\FADS-SW-Python\FGVs\FGV_Python-INI.vi</p>
	<p align="center">FGV_Stop.vi</p> <p>Operation   Stop Button OUT</p> <p>Stop Button IN   Stop Button IN</p> <p>Error IN (no error)   Error OUT</p> <p>This FGV stores the Boolean value to control STOP of Progress Ring While Loop.</p> <p>C:\FADS-SW-Python\FGVs\FGV_Stop.vi</p>
	<p align="center">Experiment Parameters to JSON.vi</p> <p>Experiment parameters   Experiment Parameters to JSON</p> <p>Histogram Y axis   Experiment Parameters to JSON</p> <p>C:\FADS-SW-Python\PDF-report\Experiment Parameters to JSON.vi</p>
	<p>FADS Experiment parameters - divided.ctl</p> <p>C:\FADS-SW-Python\Controls\FADS Experiment parameters - divided.ctl</p>
	<p>Histogram Settings.ctl</p> <p>C:\FADS-SW-Python\Controls\Histogram Settings.ctl</p>
	<p>Histogram Y axis.ctl</p> <p>C:\FADS-SW-Python\Controls\Histogram Y axis.ctl</p>

CTL POST-S ANALYS.	Post-sorting_analysis.ctf C:\FADS-SW-Python\Controls\Post-sorting_analysis.ctf
CTL PRE-S ANALYS.	Pre-sorting_analysis.ctf C:\FADS-SW-Python\Controls\Pre-sorting_analysis.ctf

D Electronic supplement

The electronic supplement consists of supporting data for the bachelor thesis. The hierarchy of root directory is here:

```
/.-----the root directory of the attached archive
├── Cinderella Analyser .....FADS data analyzing software
│   ├── Controls
│   ├── Demo Data ..... Folder with data for software testing
│   │   ├── Sorting_timetrace_100kHz_1.tdms
│   │   ├── Sorting_timetrace_100kHz_1.tdms_index
│   │   ├── Sorting_timetrace_100kHz_2.tdms
│   │   ├── Sorting_timetrace_100kHz_2.tdms_index
│   │   ├── Sorting_timetrace_100kHz_3.tdms
│   │   └── Sorting_timetrace_100kHz_3.tdms_index
│   ├── Display Data
│   ├── Documentation
│   │   └── Cinderella Analyser - Workflow and documentation.pdf
│   ├── Export Data
│   ├── FGVs
│   ├── PDF-report
│   ├── Progress-Ring
│   ├── Python-code
│   │   └── timetraces_checker.py ..... Python functions for Cinderella Analyser
│   ├── Python-nodes
│   ├── Main.vi
│   ├── Cinderella Analyser.lvproj
│   ├── Cinderella Analyser.lvlps
│   └── Cinderella Analyser.aliases
├── Reports .....PDF reports from analyzing software
│   ├── 2023-04-18 Pre-Sorting Analysis.pdf
│   └── 2023-04-18 Post-Sorting Analysis.pdf
└── readme.txt
```

D.1 LV-Project

Software section focuses on the Cinderella analysing software that was developed as a part of a bachelor thesis and used in experiments for calculations.

D.2 Reports

This folder consists of 2 reports in PDF generated by analyzing software. Reports include experiment parameters that were used. There are full reports from pre-analysis and post-analysis from the InDel sorting with 1,2-Dibromethane,.